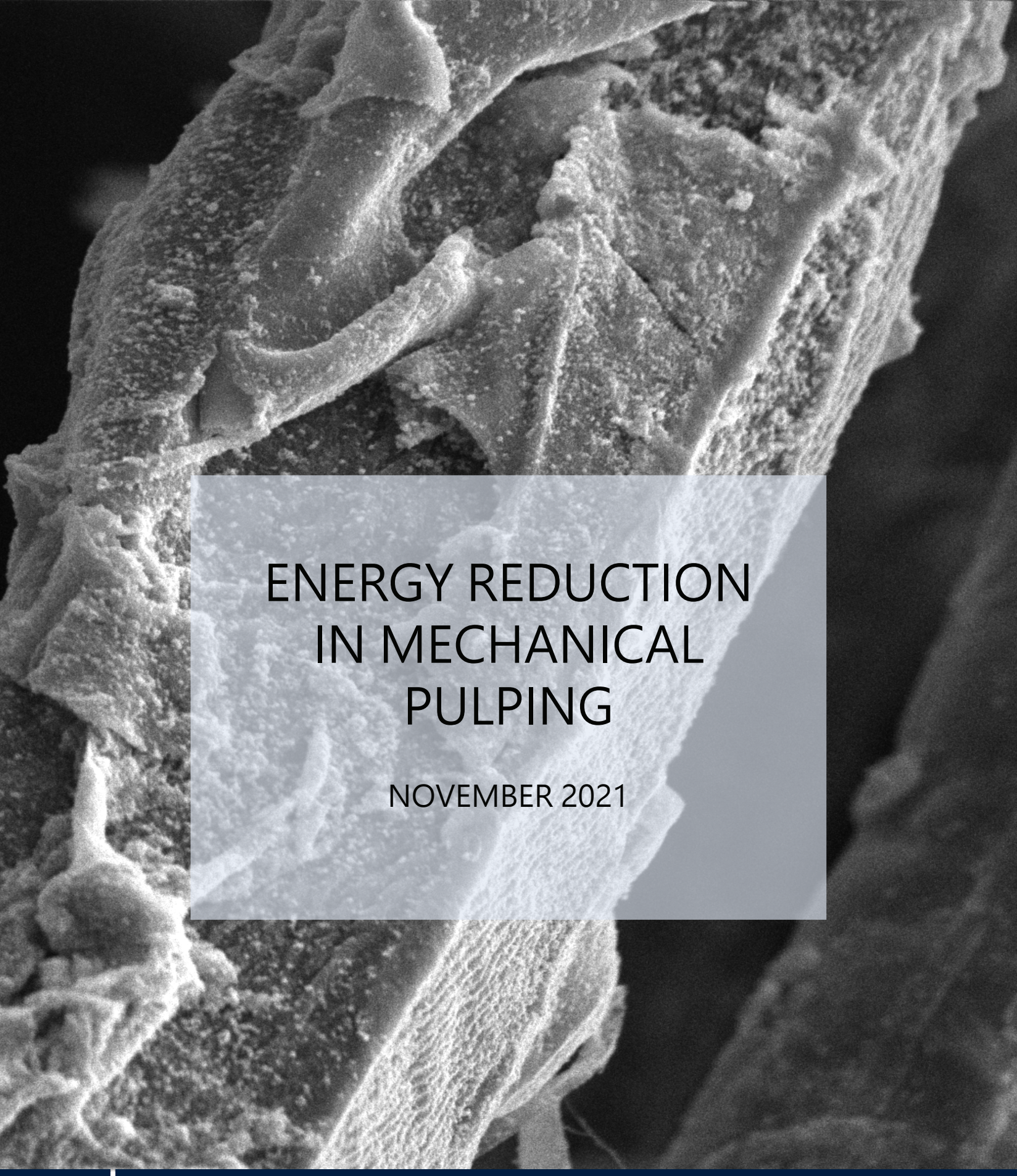

ENERGY REDUCTION IN MECHANICAL PULPING

NOVEMBER 2021

THE UNIVERSITY OF BRITISH COLUMBIA

WELCOME MESSAGE

Dear partners in the Energy Reduction in Mechanical Pulping research program,

I am pleased to update you on the latest developments in the program. Since our last newsletter, we held our second online Steering Committee meeting early this summer where graduate students, and postdocs presented project updates on the development of the third phase. This was our second time successfully meeting in an online format, and we thank you again for your support and the valuable feedback provided to the research team.

In good news for the team, Matthias Aigner has a date for his Doctorate Oral Defence early December. On the following pages, I invite you to read Matthias's last summary update on his doctoral work and the team's research progress since our last newsletter. We look forward to discussing this project milestones in our next Steering Committee meeting on November 16th, happening online. We hope to see you there.

As the year progresses, we have also had personnel updates with new highly qualified personnel joining the consortium, and some farewells. Reanna Seifert, Laboratory Technician based at the PPC left the team early October to continue her career on the island. We thank Reanna for all the great contributions to the ERMP team, and wish the best on her future endeveours. A new Laboratory Technologist, Norman Roberts has joined the team, and is now responsible for running the pilot plan facility and supporting the papermaking lab. Additionally, we have also welcomed Co-op students, Dua E Naqvi and Samuel Brown at the PPC. I invite you to review pages 32 and 33 for brief introductions to our new team members and their backgrounds.

With the ease of travelling for next year, I would like to also extend an invitation for the International Mechanical Pulping Conference (IMPC) happening in Vancouver from June 5th to the 8th. Our next Steering Committee meeting will be planned around the IMPC 2022, and we hope you can mark your calendars to attend both events. We will update you once a date is confirmed.

Wishing you the best and good health, hoping we can meet in person soon.

Mark Martinez, Ph.D., P. Eng.,
Professor of Chemical and Biological Engineering, UBC
Principal Investigator, ERMP Research Program
Director of Advanced Papermaking Initiative, API

CONTRIBUTORS

Matthias Aigner
Rodger Beatson
Samuel Brown
Yankai Cao
Siwei Chen
James Drummond
Mengqi Fang
Elisa Ferreira
Mariana Frias de Albuquerque
Samira Gharehkhani
Bhushan Gopaluni
Pierre Betu Kasangana
Sudipta Kumar Mitra
Liyang Liu
Mark Martinez
Claire Maulit
Dua E Naqvi
James Olson
André Phillion
Scott Renneckar
Norman Roberts
Laurel Schafer
Reanna Seifert
Aurélien Sibellas
Boris Stoeber
Heather Trajano
Daniela Vargas Figueroa
Peter Wild
Cameron Zheng

PRODUCTION EDITOR and DESIGNER
Daniela Vargas Figueroa

MAILING ADDRESS
UBC Pulp and Paper Centre
2385 East Mall
Vancouver, BC V6T 1Z4

CONTACT
Program Manager
Daniela Vargas Figueroa
daniela.figueroa@ubc.ca
604-827-2390

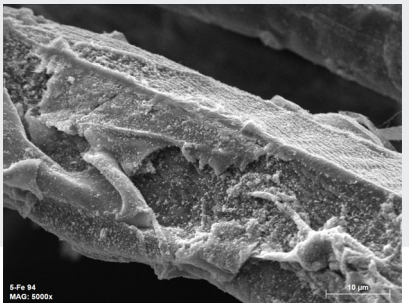

CONTENTS

RESEARCH UPDATES

PROGRAM UPDATES

CONTACTS

ON THE COVER

Scanning Electron Image of a CTMP handsheet labelled with Fe_2O_3. Image at 5000x magnification. Photo credit to Dr Elisa Ferreira from Project 3.1.

PROJECT 1.1

LC REFINER BAR FORCE BASED CONTROL STRATEGIES

Authors: Matthias Aigner, Samira Gharehkhani, James Olson, Peter Wild

Background

In previous work by researchers at the University of Victoria, a custom piezo-ceramic force sensor was developed to measure local shear and normal forces applied to the refiner bars. This sensor, shown in Figure 1(b), has a probe that replaces a short length of a refiner bar and that is sensitive to forces that are: (1) normal to the axial facing surface of the refiner bar and (2) normal to the long axis of the refiner bar and in the plane of the axial facing surface of the refiner bar, Figure 1 (a). These forces are referred to as normal force and shear force, respectively. Sensors based on this design have been used in trials in a variety of high consistency (HC) [1] and low consistency (LC) refiners [2], [3].

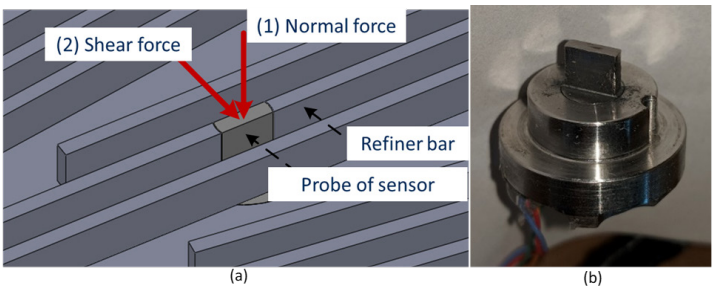

Figure 1. Force sensor set up (a) the direction of the measurable forces. (b) one of the bar force sensors.

In the most recent phase of this research, six sensors were installed in an Andritz TwinFlo 52" LC-tertiary refiner at the Catalyst, Paper Excellence mill in Crofton BC. The goal of this trial is to investigate: the radial distribution of forces, the effect of operating conditions on these forces; and, as in the previous work at UBC, the profile of forces during bar passing events. Three sensors are situated in each stator plate at three radial positions. In Figure 2(a), the positions of the sensors are indicated on a CAD drawing of a refiner plate. Figure 2(b) is a photograph of the back of the stator plate, showing the housings that protect the sensors from the environment inside the refiner.

The sensors were commissioned on January 8th 2020 at during the installation of new plates and remained operational until the plates reached their end of lifetime in July 2021, after 9400 h of operation. The sensors recorded forces during day-to-day operation and, in addition, trials were conducted to collect force data as the refiner load is increased (i.e. power curves).

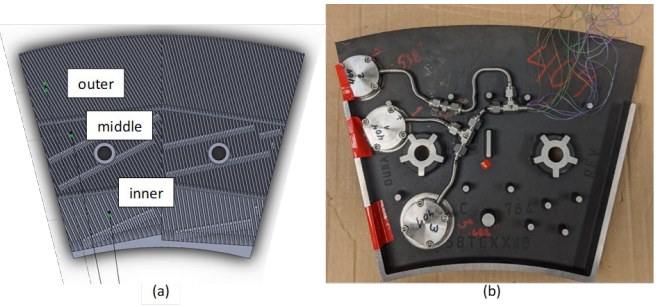

Figure 2. (a) CAD drawing of Stator plate. Sensor positions are indicated. (b) Picture of the stator plate back. Housing of sensors and wiring visible.

Long term force profiles and plate wear

Previous work by our group, in the test refiner at UBC, shows a transition from a single force peak during a bar-passing event to two peaks and that this transition corresponds to the onset of fiber cutting [4]. This behaviour was also found in power curve trials at the Crofton refiner. Based on these results, the term dual peak ratio was introduced to describes the proportion of dual peak events recorded out of all recorded bar passing events at a given refining condition [5]. This value is thought to describe the prevalence of corner force.

The dual peak ratio data is presented in Figures 3 to 6 for the outer, mid, inner tail-end positions and the inner drive-end position, respectively. Each data point presents the average value for 24 hours of run time. Included in the graphs are linear trend lines for the full plate run time to show the general trend of the data.

Analysis of the dual peak ratio shows, for all sensors, a decrease trend over the duration of the trial. For the outer sensor (tail-end) the ratio is high in the first 1000 hours and then falls off quickly (Figure 3).For the mid sensor the dual peak ratio is high until about 2000 hours and then falls continuously after that (Figure 4). The dual peak ratio for the inner sensor on the tail-end is initially small compared to the other sensors but, like the other sensors, falls off after 2000 hours (Figure 5). The inner sensor on the drive-end shows similar behaviour to the inner sensor on the tail-end but its dual peak ratio is consistently twice as high (Figure 6).

PROJECT 1.1

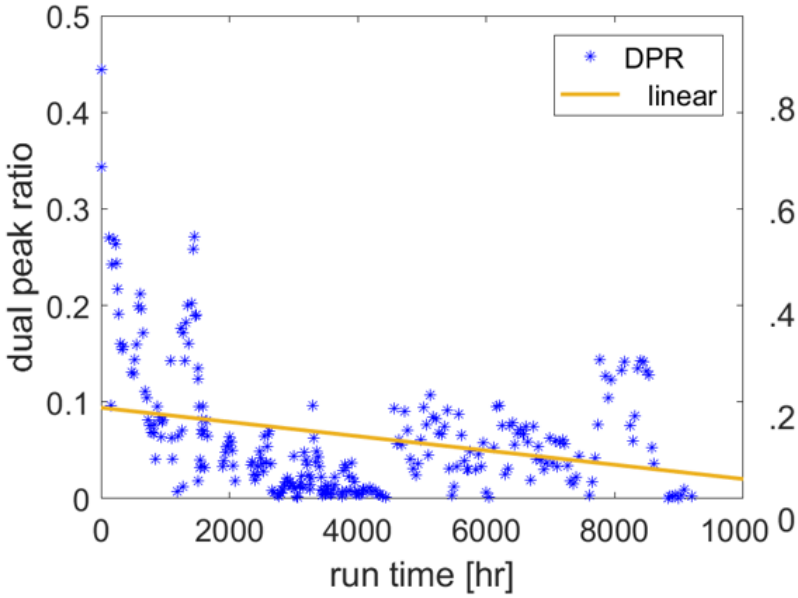

Figure 3. Outer sensor position on the tail-end side - Dual peak ratio (DPR). Values indicate the 50th percentile for each respective day.

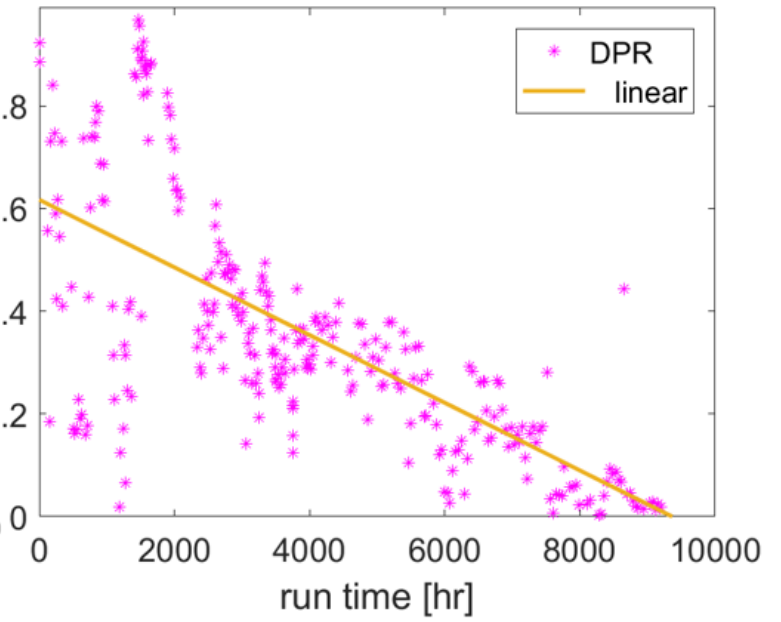

Figure 4. Mid sensor position on the tail-end side - Dual peak ratio (DPR). Values indicate the 50th percentile for each respective day.

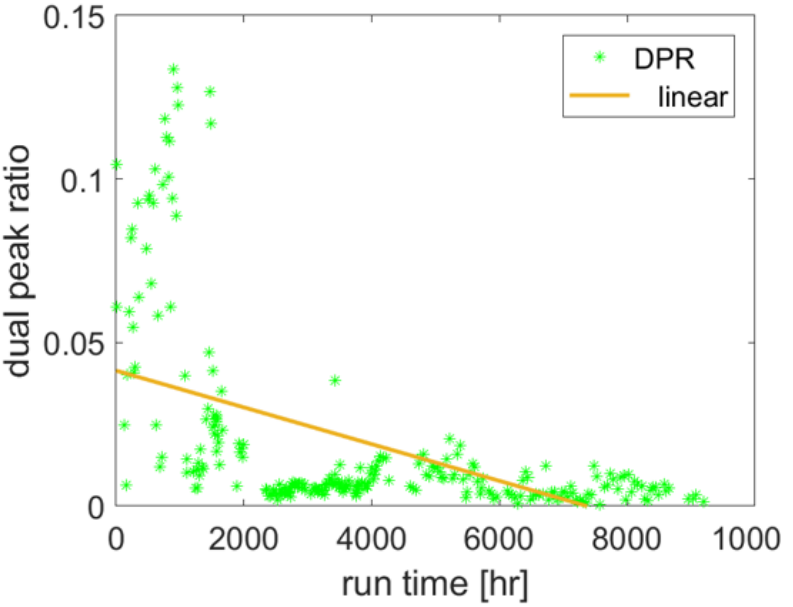

Figure 5. Inner sensor position on the tail-end side - Dual peak ratio (DPR).. Values indicate the 50th percentile for each respective day.

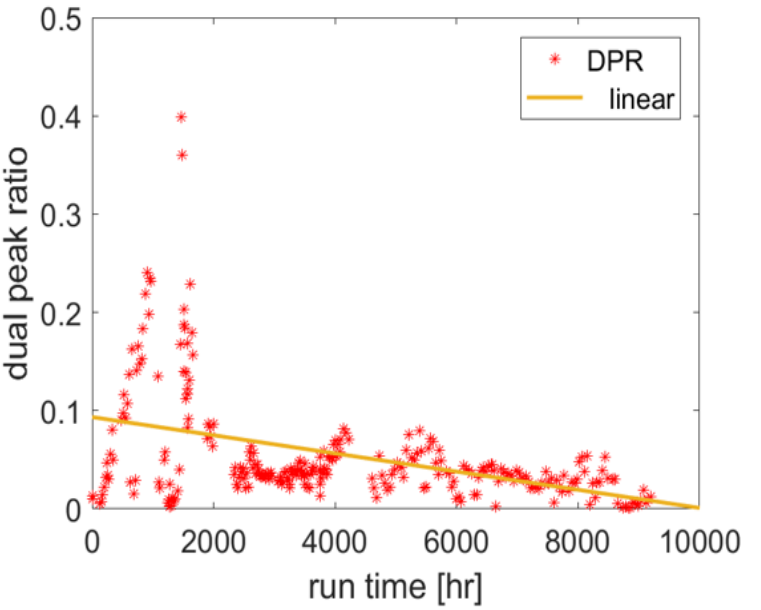

Figure 6. Inner sensor position on the drive-end side - Dual peak ratio (DPR). Values indicate the 50th percentile for each respective day.

PROJECT 1.1

Fiber length and freeness analysis of the discharge pulp samples is presented in Figure 7(a) and (b) over the run time of the refiner plates. These data points are from individual trials (i.e. power curve trials) conducted, at intervals, over the run time of the refiner plates. Fiber length is presented as length reduction relative to the feed fiber length in percent and freeness is presented as freeness reduction relative to the feed freeness. Figure 7 (a) shows a decrease in the fiber length reduction over the duration of the plate installation, except over the first 1000 hours, where there is an initial increase of the fiber length reduction. Figure 7 (b) shows a similar story for the freeness reduction. Where for the same refiner load the reduction in freeness is lower later in the plate life. The exception is again the first 1000 hours where the freeness reduction increases.

For the same refiner load, fiber length reduction and freeness reduction are lower at the end of plate life, compared to earlier in the plate run time, as shown in Figure 7. This result is consistent with the literature which shows that rounded bar edges and decreased bar height results in longer fibers [6] and higher freeness [7] at the same refiner load level, relative to fibers refined with new plates.

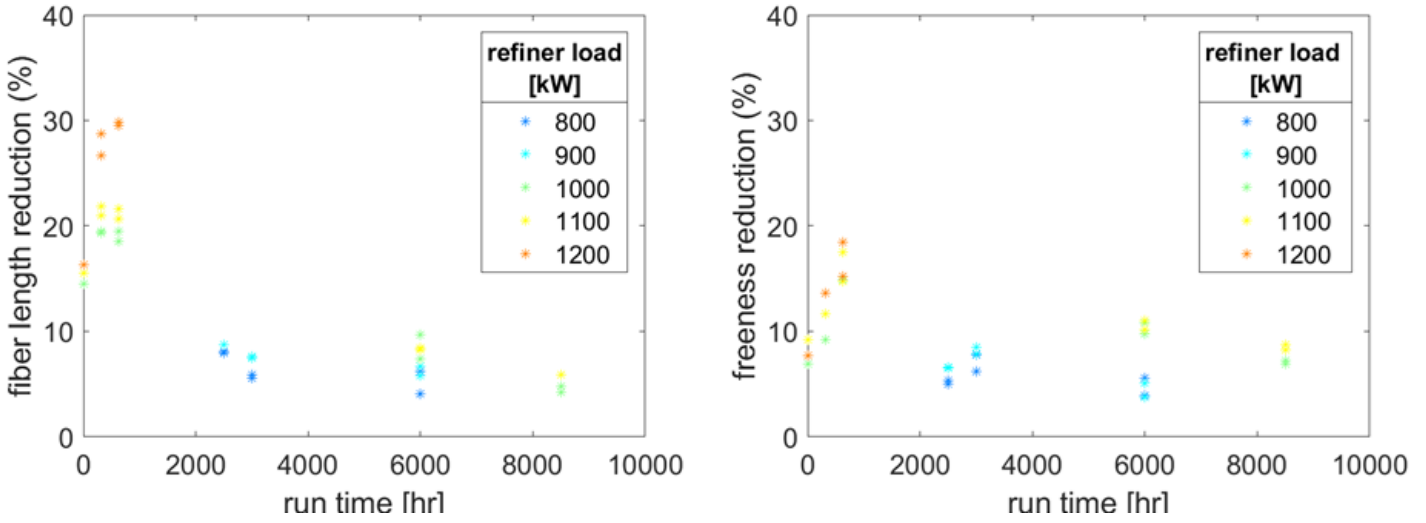

(a) **(b)**

Figure 7. Discharge fiber length decrease (a) and Freeness reduction (b) in percent plotted over the run time of the refiner plates. Colors indicate refiner load with 800 kW in blue and 1200 kW in red.

All sensors show a decrease in the dual peak ratio as the run time of the plates increases. As discussed earlier, dual peak ratio has been shown to correlate with the prevalence of the corner force during bar passing events [5]. Therefore, the decrease in the dual peak ratio indicates a decrease in the prevalence of the corner force for all sensors. At the same time, the measured bar edge radius increases over the life of the plate. These results suggest that the rounding of the leading edge of the bar decreases the prevalence of the corner force in refining.

The results in this study further suggest that the prevalence of the corner force declines while the bar height declines. It is further shown that, throughout the trial, the dual peak ratio is highest at the mid sensor position. In previous work, a high dual peak ratio was shown to indicate the prevalence of corner force [5]. As the bar height reduction at the mid position is also high, it is concluded that the higher prevalence of corner force at the mid position results in higher plate wear at the mid position.

PROJECT 1.1

Future work

Further analysis of the data acquired from the Crofton mill is planned. Special focus will be on the shear force data. The purpose of this analysis is to find patterns and similarities between normal force profiles and shear force profiles.

In the near future, the group will also conduct fundamental and experimental studies to investigate the effect of plate pattern and pulp furnish on bar forces and on the onset of fiber cutting. Here, the focus lies in validating the bar force estimation model proposed by Kerekes and Meltzer [8]. Moreover, the aim is to determine force and SRE levels where fiber shortening does not exceed a target level. These results will be compared to prior findings [8]. In addition, Kerekes and Meltzer reported that the target level of fiber shortening may be met at higher forces, but they did not have access to sufficient data to specify the conditions when this may happen. Our future trails including novel plate designs might provide an opportunity to extend the knowledge in this regard.

References

1. D. Olender, P. Francescutti, P. Wild, and P. Byrnes, "Refiner Plate Clash Detection Using an embedded Force Sensor," Nordic Pulp and Paper Research Journal, vol. 22, no. 1. pp. 124–130, 2007.
2. B. Prairie, P. Wild, P. Byrnes, D. Olender, D. W. Francis, and D. Quellet, "Forces during bar-passing events in low consistency refining: Effects of refiner tram," Pulp Pap. Canada, vol. 108, no. 9, pp. 34–37, 2007.
3. R. Harirforoush, J. Olson, and P. Wild, "Indications of the onset of fiber cutting in low consistency refining using a refiner force sensor: The effect of pulp furnish," Nord. Pulp Pap. Res. J., vol. 33, no. 1, pp. 58–68, 2018.
4. M. Aigner, J. Olson, and P. Wild, "Measurement and interpretation of spatially registered bar-forces in LC refining," Nord. Pulp Pap. Res. J., vol. 35, no. 4, pp. 600–610, Nov. 2020.
5. M. Aigner, J. Olson, Y. Sun, and P. Wild, "Interpretation of force profiles in mill-scale LC refining, accepted, awaiting publication," Nord. Pulp Pap. Res. J., 2021.
6. K. Koskenhely, K. Nieminen, E. Hiltunen, and H. Paulapuro, "Comparison of plate and conical fillings in refining of bleached softwood and hardwood pulps," Pap. ja Puu, vol. 87, pp. 458–463, 2005.
7. J. Rihs, "Low consistency refining-theory vs practice," in 3rd International Refining Conference, 1995.
8. R. J. Kerekes and F. P. Meltzer, "The Influence of Bar Width on Bar Forecs and Fibre Shortening in Low Consistency Pulp Refining," Nord. Pulp Pap. Res. J., vol. 33, no. May, pp. 1–13, 2018.

PROJECT 1.2

PULP QUALITY AND MODELING AND PROCESS OPERATING REGION EVALUATION IN THE THERMOMECHANICAL PULPING PROCESS

Authors: Mengqi Fang, Bhushan Gopaluni, Yankai Cao.

Background

In the Chemi-Thermomechanical Pulping (CTMP) process, the pulp refining processes, including the high consistency and reject refining, are considered the core operating units due to their direct effect on the pulp properties. Significant research has been done to identify the correlations between the refiner operating conditions and product properties with the hope of improving the operational efficiency. We are interested in optimizing the total specific energy (TSE) consumption while maintaining the pulp properties (Harinath, Biegler and Dumont 2011). This optimization requires a high-fidelity model that relates various process variables with TSE. However, due to the complicated, dynamic and time-varying characteristics of refining processes, building such a model is not an easy task. Therefore, as a first step, we developed different types of models and compared them to identify the best among them. Using these models, an ideal set of operating conditions were identified for the manipulated variables. Finally, the real-time operating performance of the entire refining process is summarized according to the estimated pulp quality and the potential TSE reduction.

Figure 1 below summarizes our approach which includes four stages. The process operating variables, frequently sampled pulp properties, such as freeness, and infrequently sampled handsheet properties, such as tensile, are modeled separately. The modeling procedures and the related performance measures are presented below in Parts 1 & 3. Using these models, we developed an approach for evaluating various operating regions and it is explained in Part 2. A reliability analysis of the models is also developed and presented in Part 4.

Results

Part 1: Modeling of frequently sampled pulp properties

In order to model the correlation between the process operating variables and the pulp properties, a simple but effective model structure has been employed and updated every sampling instant by using historical data in a fixed moving window. Two frequently sampled pulp properties are selected as the model outputs and the following ARX models are employed, where q_1 and q_2 represent the two pulp properties and X indicates all the selected process operating variables with time delay d. β_1 and β_2 are two model parameter vectors which are estimated and updated at every sampling instant.

$$q_1(t) = [q_1(t-1), q_2(t-1), X(t-1:t-d), 1] \cdot \beta_1(t-1)$$

$$q_2(t) = [q_1(t-1), q_2(t-1), X(t-1:t-d), 1] \cdot \beta_2(t-1)$$

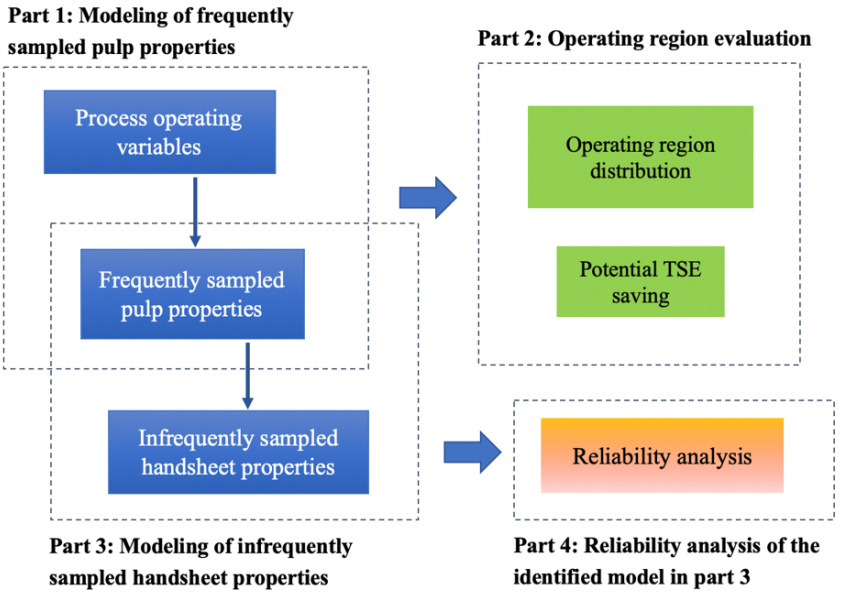

Figure 1. The workflow of this study.

PROJECT 1.2

The performance of the estimated models is validated on the real mill operating data set. As shown in Figure 2, the model output and the actual measurements are highly correlated and the normalized RMSE of q_1 and q_2 are computed as 0.0215 and 0.1582, respectively, which indicates a satisfactory modeling performance.

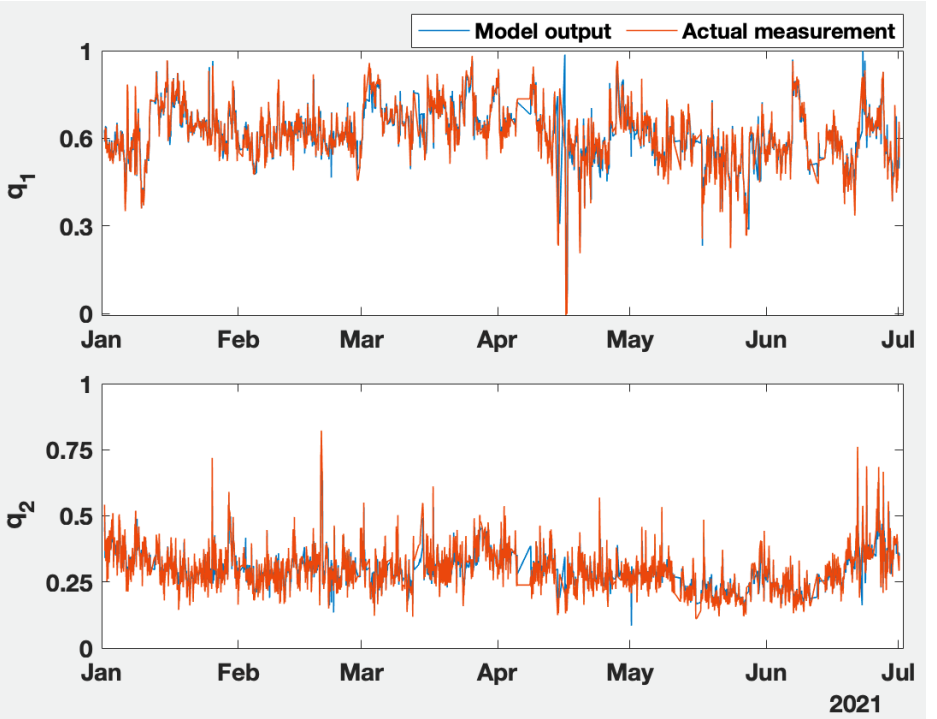

Figure 2. Model validation performance of the two selected pulp properties after normalization.

Part 2: Operating region evaluation

Based on the above ARX models, one can explore the measurement space of selected process operating variables by generating uniformly distributed random samples as model inputs. Then the model outputs q_1 and q_2 are evaluated based on the product property constraints.

Figure 3 illustrates one way to segment possible pulp quality regions, where q_1 is expected to lie between the q_1 upper and lower bounds, and q_2 is expected to be no larger than the designated q_2 upper bound. In this case, the labeled green region 1 is the desired pulp quality region, whereas the other pulp quality regions labeled by different colors are to be avoided. We are interested in finding the best way to distribute TSE between the primary and secondary refiners. Using α to denote the fraction of TSE applied to the primary refiner, we can write the following constraints:

$$SE_{p,lower} \leq TSE \cdot \alpha \leq SE_{p,upper}$$
$$SE_{s,lower} \leq TSE \cdot (1-\alpha) \leq SE_{s,upper}$$

where $SE_{p/s,upper}$ and $SE_{p/s,lower}$ indicate the upper and lower bound of primary and secondary refiner specific energies, respectively.

After comprehensively exploring the sample space of TSE and α, a 2D feasible map is created and illustrated in Figure 4. Here, corresponding to the TSE and α values, the model predicted $(\hat{q}_2, \hat{q}_1)$ pair is labeled by the region number and color according to Figure 3, and the black diamond shows actual process operating status and pulp quality. The distribution of multiple regions in Figure 4 is summarized in Table 1, which can also be interpreted as the probability of the process spending time in that region. In other words, the longer a process spends in region 1, the more likely that it produces desired pulp products. Additionally, the dark shaded green area in Figure 4 represents operating regions with lower TSE consumption.

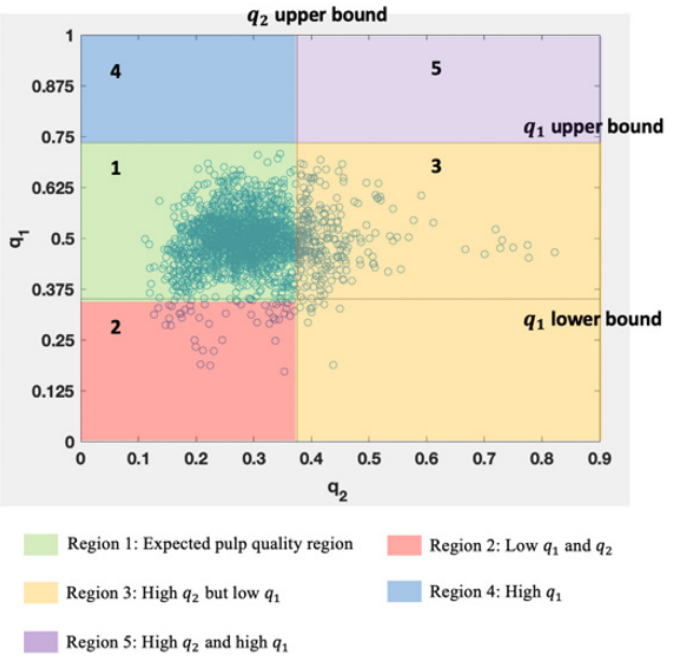

Figure 3. An illustration of pulp quality region segmentation

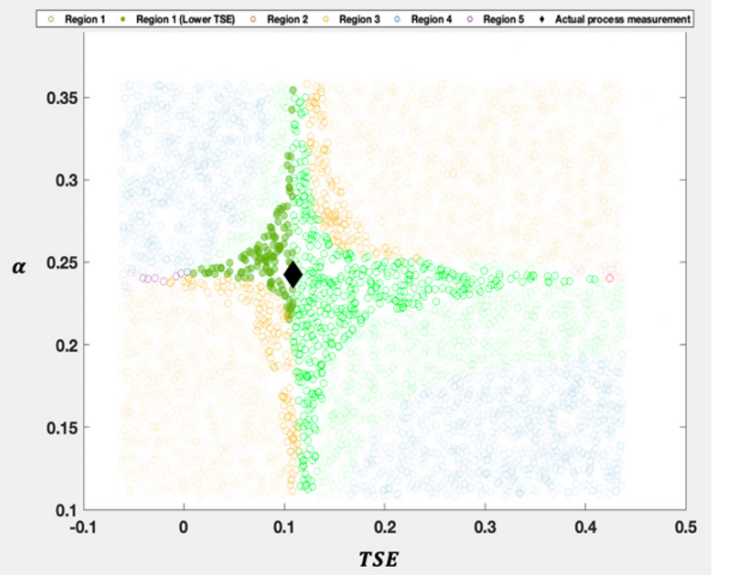

Figure 4. 2D feasible map

Table 1. The distribution of multiple pulp quality regions.

Quality region	Region 1	Region 2	Region 3	Region 4	Region 5
Percentage	68.32%	0.12%	30.75%	0.12%	0.69%

Part 3: Modeling of infrequently sampled handsheet properties

Similar to the modeling strategy explained in Part 1, linear model structure is employed when performing modeling of infrequently sampled handsheet properties. The model inputs and outputs are included in the following equations, where h₁ and h₂ represent the selected handsheet properties, Q indicates all the other infrequently sampled quality variables, and q₁ is the frequently sampled pulp property variable. The model input features are selected and computed following the PhD dissertation (Qian 1996). With this model structure, a PLS regression model (de Jong 1993) is employed and model parameters are estimated. The statistics of model performance are summarized in Table 2.

$$z(t) = [h_1(t-1), h_2(t-1), Q(t-1), q_1(t)]^T$$

$$h(t) = [h_1(t), h_2(t)]^T$$

Table 2. The statistics of model prediction performance.

Statistics	R^2 value	Normalized RMSE	Correlation coefficient of the model output and actual measurement
Handsheet property h_1	0.5705	0.1334	0.7649
Handsheet property h_2	0.4930	0.0839	0.7069

PROJECT 1.2

Part 4: Reliability analysis of the model identified in Part 3

The identified model in Part 3 is used to generate real-time predictions of the infrequently sampled handsheet properties, which are normally sampled in days or even weeks. Therefore, it is important to quantify the reliability of this model. By using probabilistic models between the prediction error e and the frequently sampled model input q_1, a novel reliability measurement index is proposed in the following equation:

Table 3. The reliability analysis validation.

Prediction error	$R_t > 0$	$R_t \leq 0$
$\|e\| \leq th$	72.26%	51.61%
$th < \|e\| < 1.5th$	16.99%	12.90%
$\|e\| \geq 1.5th$	10.75%	35.48%

$$R_t(q_1) = P(|e| \leq th|q_1, D) \cdot P(r = 0|q_1, D) - P(|e| > th|q_1, D) \cdot P(r = 1|q_1, D)$$

where th is the manually set threshold to classify the model reliability based on the absolute error value, and r denotes the reliability status of this model given q_1 and historical data D, where $r=0$ indicates the model falls into more reliable region and $r=1$ implies the model is less reliable.

When the reliability index R_t is less than or equal to zero, it indicates that the model is less reliable than for a positive R_t. As a validation, Table 3 summarizes the actual prediction error distribution with different R_t values. From this result, we can clearly observe that when $R_t \leq 0$, there are more than 35% of samples resulting in larger absolute errors, which is much higher than the errors when $R_t > 0$ case.

Conclusions and future work

Focusing on the core high consistency refining units in CTMP process, we modelled frequently sampled pulp properties and infrequently sampled handsheet properties. Using a model, the sample space of selected process operating variables is explored and evaluated by inspecting the predicted pulp qualities, and a reliability index is developed to monitor the model prediction accuracy in real time. This work has been validated using the most recent mill data. Our eventual goal is to use these tools to provide helpful guidelines on how to operate the mill so as to optimize energy consumption without compromising on the quality of the products.

References

1. de Jong, Sijmen. 1993. "SIMPLS: An Alternative Approach to Partial Least Squares Regression." Chemometrics and Intelligent Laboratory Systems 251–63.
2. Harinath, Eranda, L. T. Biegler, and Guy A. Dumont. 2011. "Control and optimization strategies for thermo-mechanical pulping processes: Nonlinear model predictive control." Journal of Process Control 21 (4): 519-528.
3. Qian, Xingsheng. 1996. "Modelling and dynamic simulation of CTMP plant." Dissertation University of British Columbia.

PROJECT 1.3

CREATING LOW ENERGY SHIVE-FREE PULPS

Authors: Rodger Beatson, Heather Trajano, Sudipta Kumar Mitra, Claire Maulit

Background

The broader objectives of this project are to: (1) generate a better understanding of the impact of chemical/biological treatments on the development of fibre and fines properties during LC refining and (2) develop economically viable low-energy processes that combine the use of such treatments with LC refining to produce printing/writing and board grades.

The aim is to study and develop chemical treatments entailing oxidative chemistry, including ozone, chlorine dioxide, along with hydrogen peroxide, to produce stronger mechanical pulp while reducing electrical energy consumption. From our previous work, we have seen that high alkalinity peroxide treatment (HAPT) of mechanical pulp can increase the strength and brightness of paper. The strong mechanical pulps produced by this process can be used to replace kraft pulp in high strength paper grades. Previous analyses support that the strength gains arise from introduction of acid groups at the surfaces of fibers and fines [1,2].

In the previous ERMP Newsletter (June 2021) we reported results from a simple settling test and imaging by X-ray tomography that showed that HAPT had a major effect on the initial consolidation of the pulp suspension and the structure of the final paper sheet.

In an effort to obtain a better understanding of the mechanism behind the strength development in HAPT, a second-stage TMP was treated in a one-stage APT process over a range of alkali charges. The effect of these treatments on the forming and pressing stages of handsheet production were investigated. We further developed a protocol to separate mechanical fibre and fines, in order to determine the relative contribution of treated fines and treated fibres to sheet consolidation and property development.

Experimental

A secondary refiner TMP (60% Spruce/40% Pine) of CSF 390 mL was treated with 4% hydrogen peroxide while varying the alkali charging from 2.5% to 6% as shown in figure 1. After washing with deionized water, handsheets were made to measure the strength and optical properties. To determine the effect of the treatments on the pressing process, pressing pressure was varied from 0 psi to 60 psi utilizing only a single press during handsheet pressing.

Separation of mechanical fibre/fines: A procedure was developed, as outlined in figure 2, that separated fines at a high enough consistency to allow for preparation of handsheets from combinations of treated fines and untreated fibres. Four thousand grams of a 0.5 % consistency pulp suspension was poured into an agitated Somerville shive separator fitted with a 200-mesh screen. The resulting pulp was washed with 20 litres of deionised water with constant agitation. The separated long fibres were collected from the top of the mesh. The collected fines suspension was allowed to settle for 24 h, then water was siphoned from the top of the suspension to increase the consistency. A second stage siphoning of water was conducted after letting the suspension settle for another 3 - 6 h.

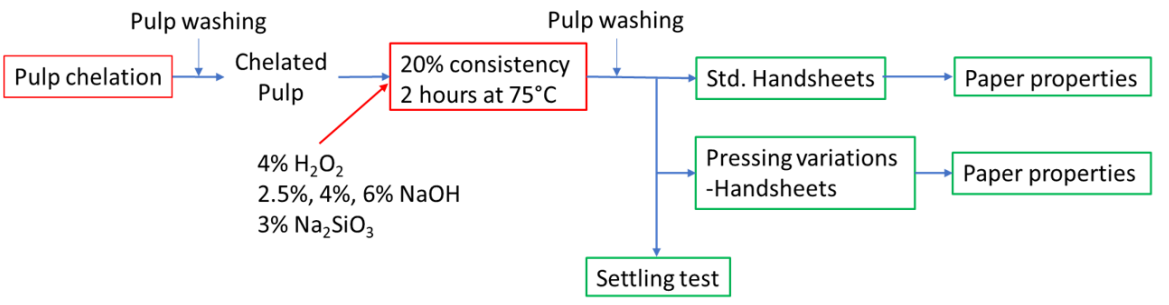

Figure 1. Experimental flowchart for alkaline peroxide treatment of mechanical pulp.

PROJECT 1.3

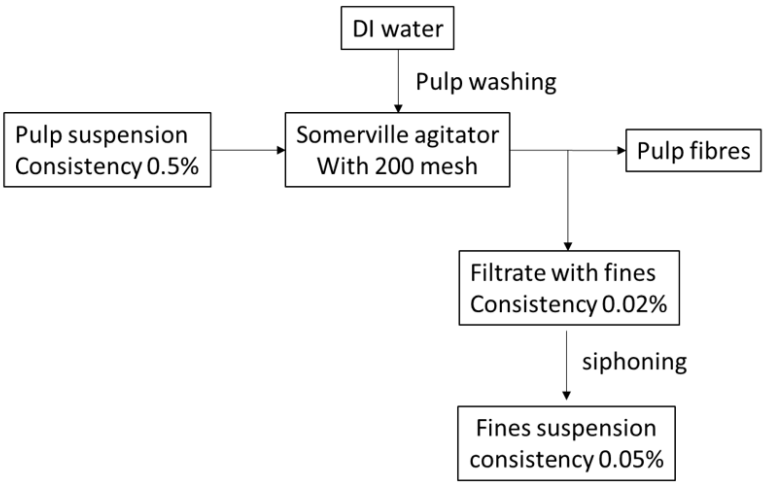

Figure 2. Experimental flowchart for fibre/fines separation

Results

In our previous work, we found tensile strength increases with alkali charge and almost doubles at 6% alkali charge, confirming that highly alkaline peroxide treatment can be used to produce high strength mechanical pulp. As reported in the previous newsletter, it was found that the settling height of pulp suspensions decreases significantly with increase in alkali percentage, indicating a strong effect of the treatment on the initial forming process.

In order to evaluate the effect of HAPT on sheet consolidation during pressing, handsheets were made using different pressing pressures and the paper properties were measured. The tensile strength increases with increasing alkali charge and pressing pressure as shown in figure 3a; there is a corresponding decrease in bulk shown in figure 3b. It is important to note that the increases in tensile and decreases in bulk, arising from increasing alkali charge, are apparent at all pressing pressures.

In figure 3a, it can be clearly seen that the tensile strength of unpressed (0 psi) 6% APT is significantly higher than that of the untreated standard pressed sample. In addition, the bulk of unpressed (0 psi) 6% APT is significantly higher than bulk of untreated standard pressed. This demonstrates that we can achieve a high bulk with relatively high tensile with HAPT process by varying pressing conditions. The plot of bulk versus tensile strength at varying pressure levels and different alkali charges is shown in figure 4, where the black dotted line represents the standard handsheets. From this figure, it is apparent that as the alkali charge in peroxide treatment of mechanical pulp is increased, a higher bulk at a given tensile strength can be achieved. As achieving a higher bulk with higher tensile is important for many products made from mechanical pulps, this process is of practical importance.

Figure 3. (a) Comparison of tensile strength with increasing pressure levels at press section at different alkali charge in alkaline peroxide treatment (b) Comparison of bulk with increasing pressure levels at press section at different alkali charge in alkaline peroxide treatment.

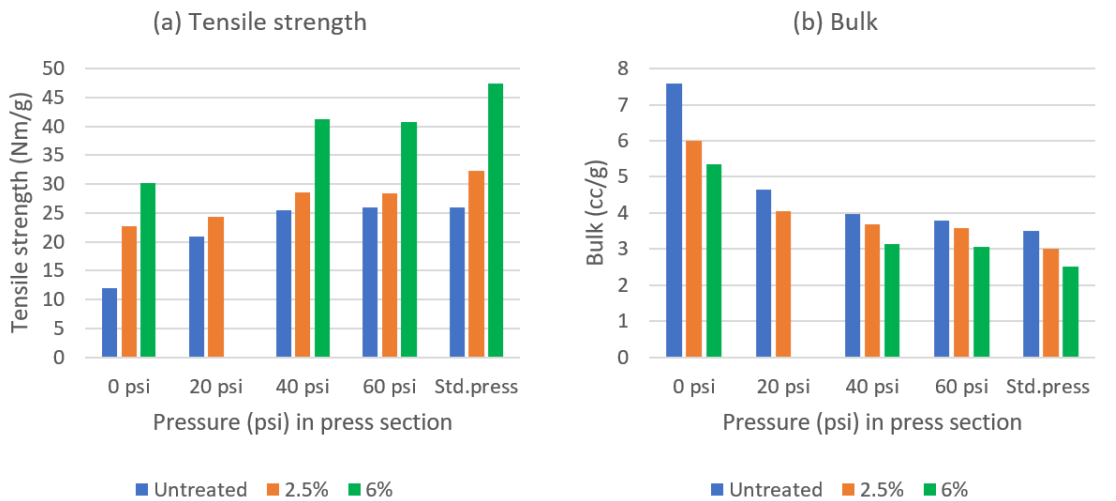

PROJECT 1.3

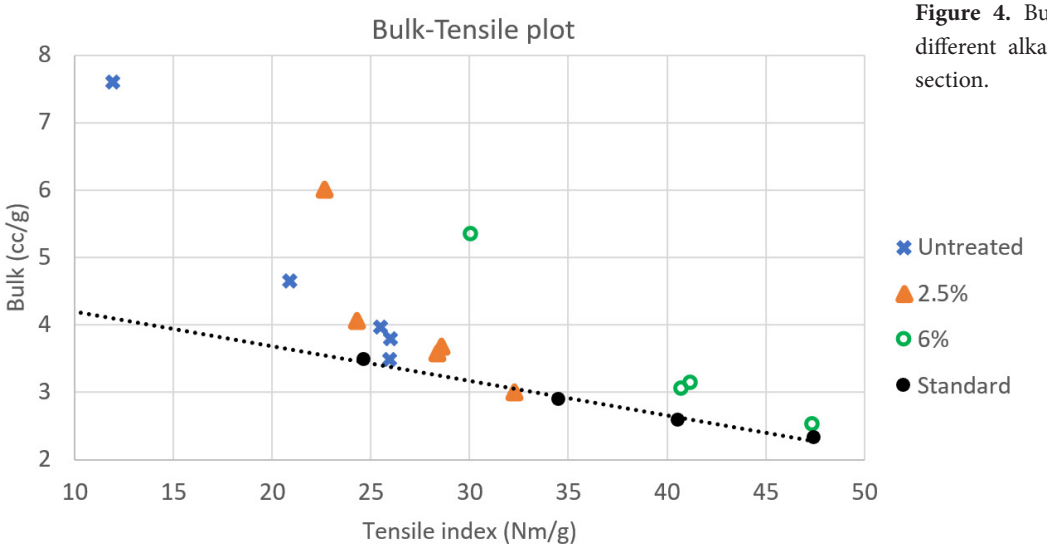

Figure 4. Bulk vs tensile strength of APT with different alkali charge at varied pressure at press section.

In summary, the chemical modifications of the fibres and fines through the HAPT process changes the behaviour of the pulp in both the forming and pressing processes.

For better understanding of the phenomenon and the driving forces behind the increases in strength of paper made with TMP treated by the HAPT process, we are studying the pulp and handsheets by microscopy. Figure 5a shows an X-ray tomography image of cross sections of handsheets of untreated and 2.5%, and 6% treated samples. Figure 5b shows the SEM images of top and bottom surface of these samples. In figure 5a, clear differences in bulk and consolidation of pulp fibres/fines between untreated and treated samples can be observed. As the alkalinity of the treatment increases the sheet density increases. This consolidation of fibres parallels our previous results from the settling of the pulp suspensions. There is also a noticeable increasing density gradient from top to bottom within the handsheets made from the treated pulps. The reason for this is unclear and will be the subject of future research.

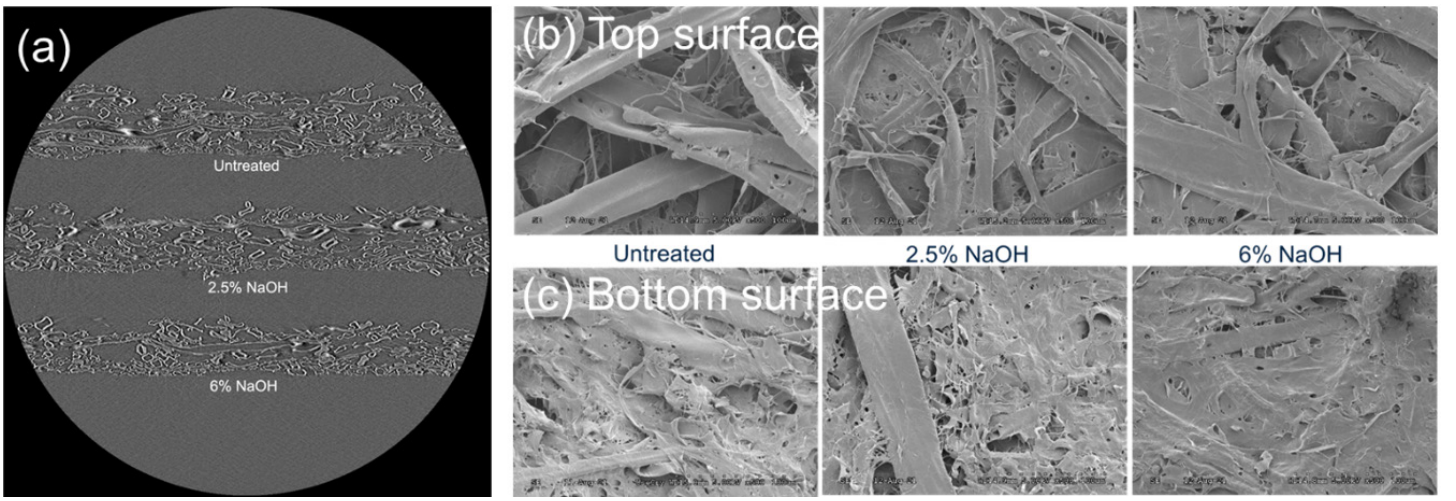

Figure 5. (a) X-ray tomography image of cross section of untreated and Alkaline peroxide treated handsheets (1.25µm resolution) (b) SEM images of top surface and bottom surface (wire side) of untreated, 2.5% and 6% APT handsheets (500 resolution)

PROJECT 1.3

In figure 5b, we get a clear picture of top surface and bottom surface (wire side) from SEM. The top surface seems to be rough, and the bottom surface seems to be much smoother than top for all the samples (untreated and treated). Further it can be observed from these SEM images, particularly for the top rough side, that more gaps and unbonded area exists in the untreated handsheet in comparison to the treated samples. These images strongly support our hypothesis that fibre/fines consolidation is driving the strength development with APT.

To evaluate the impact of HAPT treated fines on consolidation of fibre/fines and strength development, we developed a procedure to separate fines from mechanical pulp fibre as shown in figure 2. Fines separated from untreated mechanical pulp were combined with fibres from 6% APT treated mechanical pulp, and vice versa in the ratio of 30% fines to 70% fibres. Preliminary results obtained from mechanical fibre/fines study are shown in figure 6.

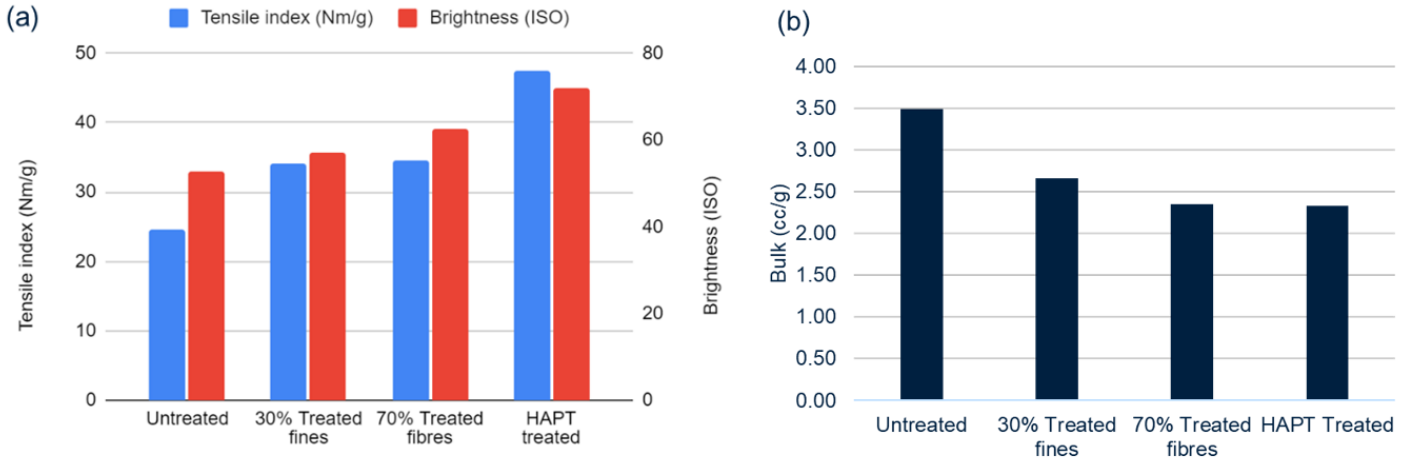

Figure 6. (a) Tensile strength and brightness of untreated, 30% treated fines/70% untreated fibre, 70% treated fibre/30% untreated fines, and Treated samples. (b) Bulk of untreated, 30% treated fines/70% untreated fibre, 70% treated fibre/30% untreated fines, and Treated samples.

Figures 6a shows the tensile strength and brightness obtained from combining treated and untreated fines with untreated and treated fibres respectively. Brightness gradually increases when a higher mass fraction of total pulp has been treated with HAPT, due the bleaching effect of the hydrogen peroxide. When treated fines were combined with untreated fibres a significant rise in tensile strength was observed. When treated fibres were combined with untreated fines a similar enhancement in tensile strength was found despite the fact that now 70% rather than 30% of the pulp had been treated. Apparently, treatment of fines plays the major role in the strength development. Further, as seen in figure 6b, a big drop in bulk occurs when untreated fines are replaced with 30% treated fines. The observation that the bulk for the sheet made from 70% treated fibres/30% untreated fines is only slightly lower than that of the 70% untreated fibres/30% treated fines indicates that the HAPT does not have a major effect on fibre flexibility.

All these observations demonstrate the role and importance of treated fines on fibre/fines consolidation and strength development. Though this is a study with only a small data set, it indicates we are moving on right path. A much clearer and better understanding will be gained when all studies are completed.

Conclusions

High alkalinity peroxide treatment of mechanical pulp increases the tensile strength. Thus, this process can be used for producing stronger pulp for grades of paper which demand high strength like flexible packaging paper grades. The results imply that majority of the tensile strength increase takes places during the forming and pressing process. Imaging by X-ray tomography and SEM provides insight into the effect of the highly-alkaline peroxide treatment on fibre and sheet consolidation. The treatment modifies the fibre/fines surface in such a way that increases the settling rate promoting fibres/fines consolidation which can be assumed to be driving force in strength development. Further, it seems that treated fines play an important role in the mechanism of strength development.

PROJECT 1.3

Future Research

In future work, the role of the HAPT fines in sheet consolidation will be further investigated through varying mixing ratios. In preparation for industrial applications of the technology, the kinetics of the strength development and effects of mill process waters will be determined. Staining and dyeing techniques for better imaging, along extractives content analysis are ongoing with collaborations with other ERMP researchers.

Other work under this project will evaluate the various chemical treatments explored in Stage I and Stage II of the ERMP program with respect to their suitability for use in different products such as paperboard, printing papers and flexible packaging.

References

1. X. F. Chang, A. Luukkonen, J.A. Olson, R.P. Beatson, “Pilot-Scale investigation into the effects of alkaline peroxide pretreatments on low-consistency refining of primary refined softwood TMP“, BioResources, 11(1), 2030-2042, 2016.
2. X. F. Chang, C. Bridges, D. Vu, D. Kuan, L. Kuang, J. A. Olson, A. Luukonen and R. P. Beatson, "Saving Electrical Energy by Alkaline Peroxide Treatment of TMP prior to Low Consistency Refining," Journal of Pulp and Paper Science, vol. 36, pp. 129-134, 2010.
3. S. Moldenius, "The Effects of Peroxide Bleaching on the Strength and Surface Properties of Mechanical Pulping," Journal of Pulp and Paper Science., vol. 10, pp. 172-177, 1984.
4. J. R. Presley and R. T. Hill, "Peroxide bleaching of (chemi) mechanical pulps," in Pulp Bleaching: Principles and Practice, C. W. Dence and D. W. Reeve, Eds. Atlanta, Georgia: TAPPI, 1996, pp. 457-489.
5. A. Korpela, "Improving the Strength of PGW Pine Pulp by Alkaline Peroxide Treatment," Nordic Pulp and Paper Research Journal, vol. 17, pp. 183-186, 2002.
6. J. Been, "A Novel Approach to Kinetic Modeling of the Hydrogen Peroxide Brightening of Mechanical Pulp," Tappi Journal, pp. 144-152, 1995.
7. P. Engstrand, B. Sjogren, K. Olander and M. Htun, "The significance of carboxylic groups for the physical properties of mechanical pulp fibers," in 6th International Symposium Wood Pulping Chemistry, 1991, pp. 75-79.

PROJECT 2.1

LIGNIN RICH FINES: SIMPLE ROUTES TOWARDS CREATION OF HYDROPHOBIC AND HYDROPHILIC FILLER ADDITIVES

Authors: Liyang Liu, Siwei Chen, and Scott Renneckar

Background

Primary fines from mechanical pulping are classified as wood particles passing through 200 mesh screen, meaning that they are less than 76 μm in size [1]. Their composition reflects the plant secondary cell wall, containing cellulose, hemicellulose, and lignin. As a significant source of lignocellulosic materials found in a waste stream, it may be possible to capture additional value to prepare next-generation materials [2-4]. Through their isolation and modification (e.g., esterification or etherification) [5], we can attempt to tune their composition and structure in obtaining plastic materials for the application from food package to 3D printing inks or coatings. [6,7]

Our previous report explained the impact of their surface hydroxyl groups on limiting the melt processing with thermoplastics. The inter-and intra- molecular hydrogen bond from functional groups limit their dispersibility in solvents and cause aggregation during melt processing.[8] Fortunately, the esterification and etherification of their surface hydroxyl groups can convert them into different types of functional groups such as hydrophobic aliphatic chains or reactive amine and carboxylic acids to enhance their properties (e.g., solubility and inject-molding).[5] For example, Hou et al. applied a mechanochemical process to add oleic acid chains on the surface of cellulose and successfully prepared melt-processable oleic acid esterified cellulose materials.[9] By performing the reaction during ball milling, this process effectively substituted the hydroxyl groups with aliphatic chains without the usage of large amounts of hazardous chemicals.

On the other hand, the cationic groups (-NH3+) or anionic groups (-COO-) can help disintegrate the cellulose fibril structures that further improves their dispersibility in the water. [10,11] In doing so, these modified compounds can be used as filler additives to enhance the wet-strength of paper sheets or have favourable application in making nano-fibrillated lignin-containing cellulose. Through the cationization of wood, Sirvio et al. added around 1.5 mmol/g cationic groups on the surface of wood sawdust that enhanced their water dispersibility significantly. A microfluidizer was then applied to separate these fibrous materials into nanocellulose fibrils capable of preparing high transparency films with improved antimicrobial and UV absorption properties. [10]

In this project, we aimed at optimizing the chemistry of surface modification route using greener conditions (low E-factor and less hazardous chemicals) and preparing fines with hydrophilic or hydrophobic performances for advanced plastics materials (e.g., 3D printing ink and food package materials).

Results

Fine characterization

Since the beginning of this project, we have received three types of fines from different producers (PPC in UBC and Holmen Corp.). Two kinds of PPC fines (0 - fine and 900 - fine) were bleached in advanced and have white colour, while the fines from Holmen Company were darker (**Figure 1**). After the lyophilization, the Klason results showed that H-fine (31.5% lignin) contained the lowest lignin compounds with a larger particle size. The refined 900-fine has more uniform particle size distribution and morphology.

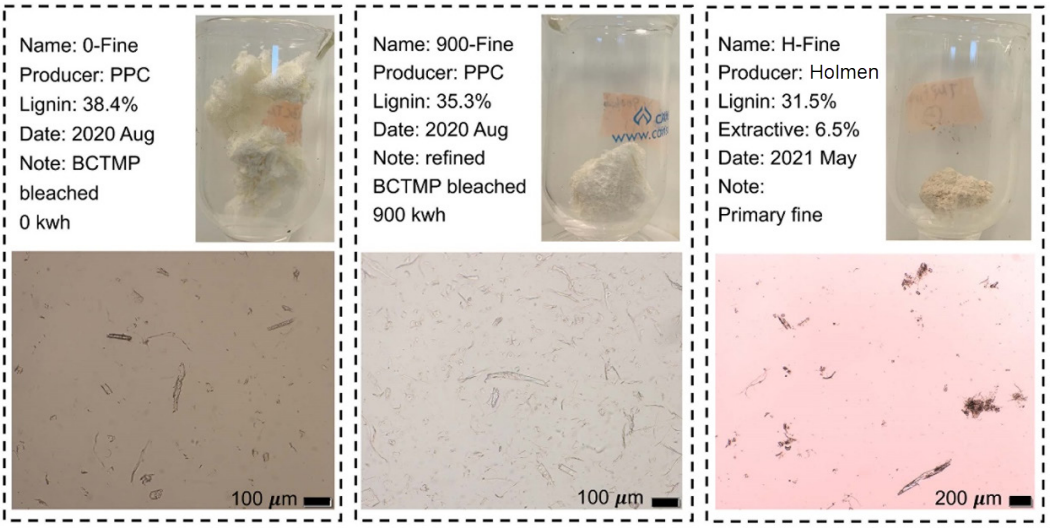

Figure 1. Characterization of mechanical fine products including micromorphology and composition

PROJECT 2.1

Hydrophobic fines

As mentioned earlier, introducing aliphatic chains on the surface of lignocellulose (especially cellulose) can potentially weaken the hydrogen bonds, disperse in hydrophobic thermoplastics, and make injectable fine-based plastics materials. So, the direct esterification was performed using oleic acid as solvent, reagent, and catalyst to esterify the hydroxyl groups in fine products. (**Figure 2a**) Our preliminary results showed that wet fine (moisture content 85%) could directly react with the oleic acid under the temperature range from 150 to 180 °C for 24- 76 hrs. FT-IR results (**Figure 2b**) demonstrated an increasing degree of esterification with the extended reaction time, i.e. the decreasing hydroxyl peak (-O-H, 3400 cm^{-1}) and increasing carbonyl peak (-C=O, 1760 cm^{-1}).

We then analyzed their thermal stability ($T_{d5\%}$, the temperature at 5% weight loss) through the thermal gravimetric curves (**Figure 2c**) because this parameter is critical to decide the thermal processing window. The $T_{d5\%}$ of the modified fine products is around 275 °C that is similar to the unmodified freeze-dried fine (FDFine), and it has little correlation with the degree of substitution (**Figure 2c up)**. Noteworthy, the increasing reaction time will resulted in a slightly lower $T_{d5\%}$ than FDFine, because changes in fine composition and cellulose crystallinity may depress their stability under higher temperature. [9] The differential thermal gravimetric curve **(Figure 2c bottom)** indicated that the OA-fine could be degraded in a range from 200 °C to 490 °C. Also, an increasing intensity for the peak around 490 °C related to the degradation of oleic acid chains that occurred with an increasing degree of esterification (FTIR results).

Due to the aliphatic side chains and ester bonds, we assume it will lead to enhanced compatibility with other linear synthetic degradable plastics (i.e. poly-Lactic Acid, PLA, one of the most popular 3D printing materials). By blending these two kinds of materials, we may reduce the overall cost and improve their specific mechanical properties (e.g., elastic properties). An Xplore extruder was utilized to prepare microfiber filaments (10% modified fine+PLA) and test their performance using uniaxial tensile tests. Unfortunately, our preliminary results indicated that the modified fine as PLA additives showed nonuniform micromorphology, concentrated stress within the cross-section and depressed PLA's mechanical performances. Additional solutions will be discussed in the section on future research.

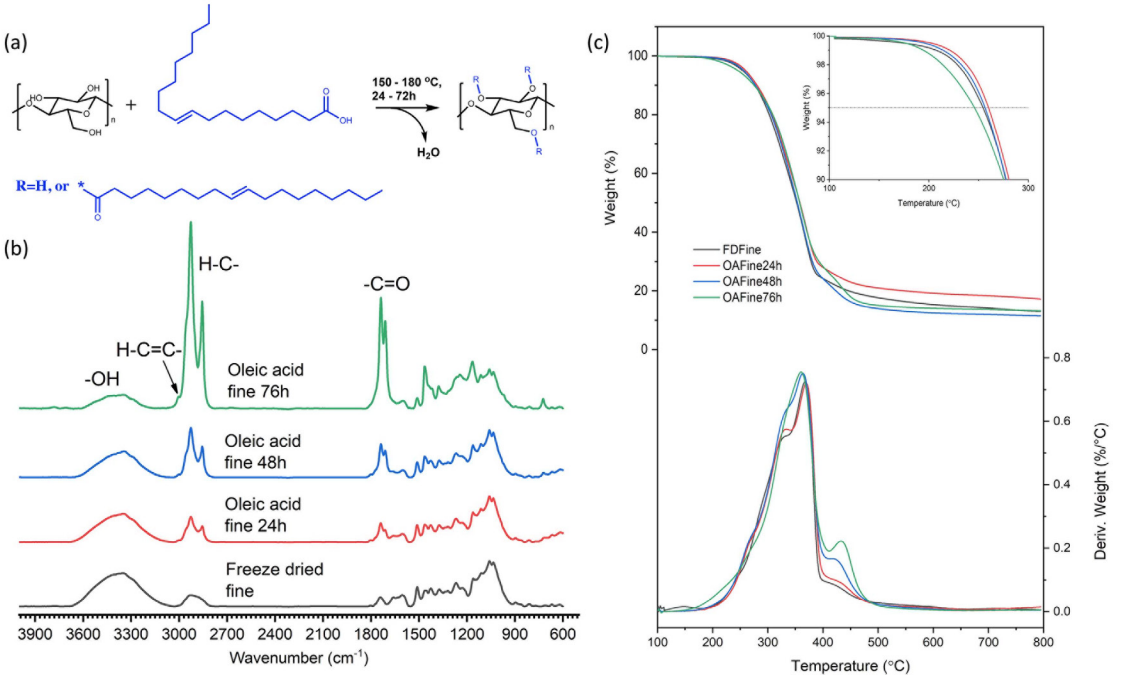

Figure 2. Mechanical pulp fines after the direct esterification with oleic acid (a, reaction scheme; b, FT-IR spectrum; c, TGA curves)

PROJECT 2.1

Hydrophilic fines

By adding cationic or anionic groups, the resulting fine can demonstrate improved dispersibility in the water. To obtain anionic fines, we apply TEMPO oxidization to selectively oxidize the primary aliphatic hydroxyl groups to carboxylic acid groups. The detailed experimental procedures were explained in Okita's paper.[12] The FT-IR results (**Figure 3**) revealed the efficiency of this modification route as an increasing amount of carbonyl peaks (1623 cm^{-1}). However, the absorption peak areas due to the lignin compounds (highlight region in **Figure 4**) also changed because the TEMPO/sodium hypochlorite will depolymerize and extract the lignin compounds during the modification process.

Future research

Hydrophobic fine: The direct esterification route was a simple way of converting the aliphatic hydroxyl groups. In addition, oleic acid sourced from renewable oil seeds will enables us to prepare more sustainable materials with a greener route (elimination of hazardous reagents). However, we need further optimize this route to get milder reaction conditions and investigate the yield, composition, and glass transition temperature during the modification. Due to lower compatibility between our modified fine and PLA than expected, two strategies were proposed to improve fine-based materials' performances: (1) we can modify the unsaturated bond in the oleic acid chain by additional functionalized route (e.g., epoxidation) to create a uniquely reactive fine product, (2) the copolymerization of the surface hydroxyl groups with other polymer precursors (such as ethylene carbonate) is another way to add polymer chains to improve the thermal processability.

Hydrophilic fines: The tempo oxidization process is an efficient way to oxidize the primary aliphatic hydroxyl groups in cellulose compounds. However, we will lose the lignin compounds that consume additional reagents and reduce the overall economic efficiency. Another interesting approach is to convert the aliphatic hydroxyl groups to primary amine (cationic groups) through etherification. A specific greener etherification route has been developed by our group recently; this route showed high efficiency in obtaining amino-functionalized lignin compounds. Our future research aims at applying this route to get amino-modified fine that does not use toxic compounds like formaldehyde. The enhanced dispersibility in water for the modified fine may allow us to prepare more hydrophilic hand sheets and advanced nanomaterials.

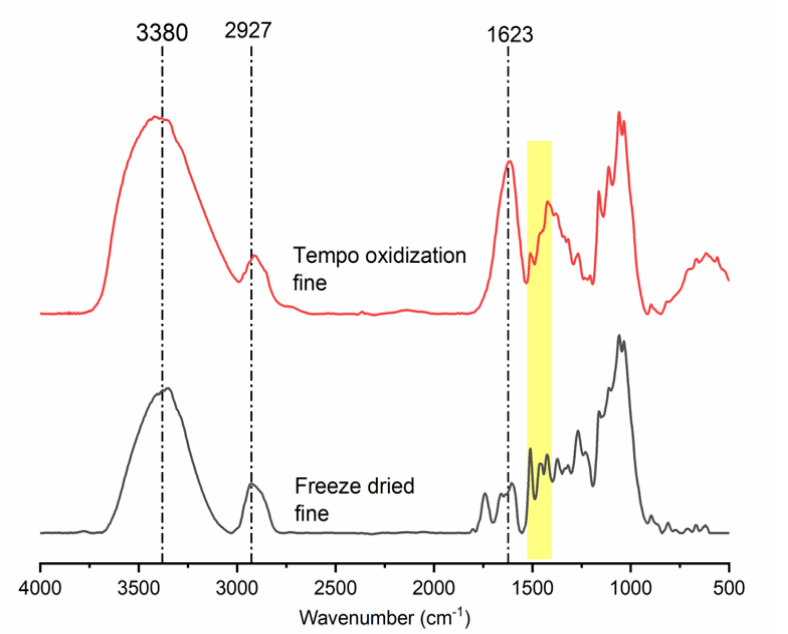

Figure 3. Mechanical pulp fines before and after the TEMPO oxidization

References

1. N. Odabas, U. Henniges, A. Potthast and T. Rosenau, Prog. Mater. Sci., 2016, 83, 574–594.
2. A. J. Ragauskas, G. T. Beckham, M. J. Biddy, R. Chandra, F. Chen, M. F. Davis, B. H. Davison, R. A. Dixon, P. Gilna, M. Keller, P. Langan, A. K. Naskar, J. N. Saddler, T. J. Tschaplinski, G. A. Tuskan and C. E. Wyman, Science (80-.)., 2014, 344, 709.
3. D. Klemm, F. Kramer, S. Moritz, T. Lindström, M. Ankerfors, D. Gray and A. Dorris, Angew. Chemie - Int. Ed., 2011, 50, 5438–5466.
4. W. G. Glasser, Front. Chem., 2019, 7, 1–17.
5. S. C. Fox, B. Li, D. Xu and K. J. Edgar, Biomacromolecules, 2011, 12, 1956–1972.
6. T. Li, C. Chen, A. H. Brozena, J. Y. Zhu, L. Xu, C. Driemeier, J. Dai, O. J. Rojas, A. Isogai, L. Wågberg and L. Hu, Nature, 2021, 590, 47–56.
7. B. Thomas, M. C. Raj, B. K. Athira, H. M. Rubiyah, J. Joy, A. Moores, G. L. Drisko and C. Sanchez, Chem. Rev., 2018, 118, 11575–11625.
8. S. Suzuki, H. Hikita, S. C. Hernandez, N. Wada and K. Takahashi, ACS Sustain. Chem. Eng., 2021, 9, 5933–5941.
9. D. F. Hou, M. L. Li, C. Yan, L. Zhou, Z. Y. Liu, W. Yang and M. B. Yang, Green Chem., 2021, 23, 2069–2078.
10. J. A. Sirviö, M. Y. Ismail, K. Zhang, M. V. Tejesvi and A. Ämmälä, J. Mater. Chem. A, 2020, 8, 7935–7946.
11. S. C. Patankar and S. Renneckar, Green Chem., 2017, 19, 4792–4797.
12. Y. Okita, T. Saito and A. Isogai, Holzforschung, 2009, 63, 529–535.

Acknowledgements

The authors thank Dr. Muzaffer Karasslan, for the assistance using the Xplore extruder to prepare plastic filaments.

PROJECT 2.2

FROM TREES TO TREATMENT FUNCTIONALIZING TMP EXTRACTIVES

Authors: Pierre Betu Kasangana, Cameron Zheng, Laurel Schafer, Heather Trajano

Background

In the TMP pulping process, wood extractives are released during debarking, bleaching and washing. A large fraction of extractives is recovered in the washing water, and another fraction, in particular volatile compounds, can be condensed in digesters.[1-2] In this emission process, monoterpenes are the most abundant, with α-pinene and β-pinene being the most common. The proportions of these extractives may be recovered as turpentine.[1]

In the washing water, the levels of fatty and resin acids depend on the process performance. [2] In particular, the pH of the process strongly affects the behavior of fatty and resin acids. [3] At high pH values, these acids dissociate and dissolve in water, depending on the temperature and the metal ion concentration. [2, 4] Therefore, the pKa values of fatty and resin acids play an important role in predicting and resolving possible problems caused by these compounds such as lower pulp quality, odor, and effluent toxicity. [5]

In our previous work, we reported the compositional analysis and the identification of lipophilic extractives in chips (wood and bark) samples provided by Meadow Lake Mechanical Pulp Inc. The current study is devoted to determining the chemical profiles of extractives in liquid samples collected from Aspen and Softwood (White Spruce and Jackpine, (30:70%)) pulping operations at Meadow Lake Mechanical Pulp Inc. In addition, an initial study of terpene functionalization in turpentine (provided by Holmen Paper AB) will be presented.

Experimental work

Each Meadow Lake liquid sample was filtered and subjected to liquid-liquid extraction with methyl tert-butyl ether (MTBE). 5 mg of MTBE extract were dissolved in 1 mL dichloromethane/pyridine mixture (9:1) and then silylated to enable sample volatilization in the GC-MS. The vial was sealed, vigorously shaken for 1 min. and heated in an oven for 30 min. at 100°C. The silylated extracts were analyzed using an Agilent 7890 gas chromatograph with 5975 mass spectrometer, equipped with a 30 m; 0.25 mm i.d.; 0.25 µm film thickness HP-5MS capillary column. The turpentine sample from Holmen Paper AB was subjected to the same analysis. The identification of extractives was performed by comparison of the spectral properties with the NIST 2.0 library.

Catalytic upgrading of turpentine proceeded in a nitrogen-filled mBraun glovebox. 1 mmol each of N-methylaniline and turpentine were added to 10 mol% of $Ta(CH_2SiMe_3)_3Cl_2$ and sodium ureate ligand dissolved in 0.3 mL d_8-toluene in a 1 dram vial. Afterwards, 0.33 mmol of 1,3,5-trimethoxybenzene was added as internal standard. The homogenous solution was transferred to a J. Young NMR tube, the vial was then rinsed with 0.5 mL d_8-toluene and transferred into the J. Young NMR tube. After sealing the J. Young NMR tube with a Teflon stopper, an ^{1}H Nuclear Magnetic Resonance (NMR) spectrum was taken prior to heating. The J. Young NMR tube was then placed in a pre-heated 145 °C oil bath. After heating, the J. Young NMR tube was analyzed by ^{1}H NMR spectroscopy to determine terpene consumption.

The anti-bacterial activity of turpentine and aminated turpentine was tested using a disk diffusion assay. Four solutions were tested with the assay: 1- turpentine, 2- aminated turpentine, 3- turpentine treated with catalyst only (control), and 4-*N*-methylaniline treated with catalyst (control). Samples 2-4 were treated with pentane to remove the catalyst by precipitation, filtered twice, and pentane was removed by rotary evaporator. The oils were used to prepare a 20 µg/mL solution in dimethyl sulfoxide. 20 µL of each solution was absorbed onto a cotton disc which was then placed onto a petri dish containing Methicillin-resistant *Staphylococcus aureus*. The petri dish was then incubated to determine qualitative anti-bacterial activity of the aminated turpentine mixture.

Results

Figure 1 summarizes the structure of lipophilic extractives identified in each liquid sample provided by Meadow Lake. Extractives from two main groups, fatty and resin acids, were found in all samples. In most samples, total resin acids were in greater concentration than total fatty acids. The amount of each compound in each sample is shown in Figure 2. Linoleic and neoabietic acids are the most abundant compounds in all samples. The concentration of linoleic acid can reach up to 900 mg/L during softwood pulping, which could be interesting for future valorization of this compound. Furthermore, removing pulp extractives may reduce odour. [2] especially linoleic acid, have been reported to be precursors of odorous compounds in pulp.

PROJECT 2.2

Autoxidation of linoleic acid produces several volatile compounds with strong odour, including hexanal. [6] Comparison of the relative rates of fatty acid autoxidation demonstrated that linoleic acid is 40 times more reactive than oleic acid.. The rapid rate of oxidation in combination with high concentrations of linoleic and its regioisomeric pair (pinolenic acid) likely result in high hexanal concentrations in TMP pulps.

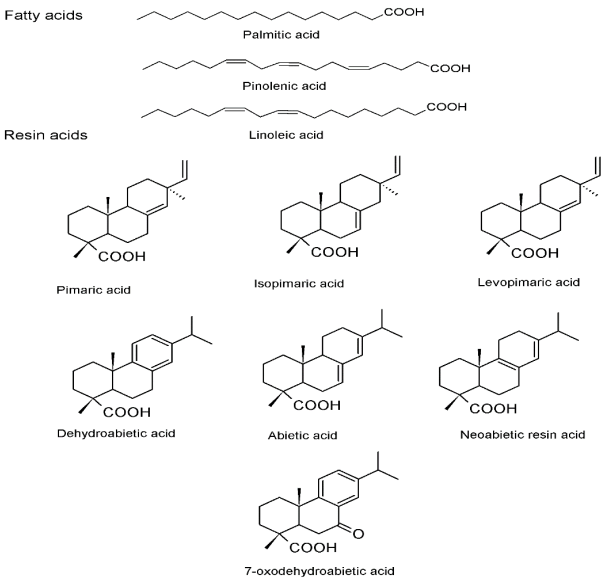

Figure 1. Structure of identified fatty and resin acids in Meadow Lake liquid samples

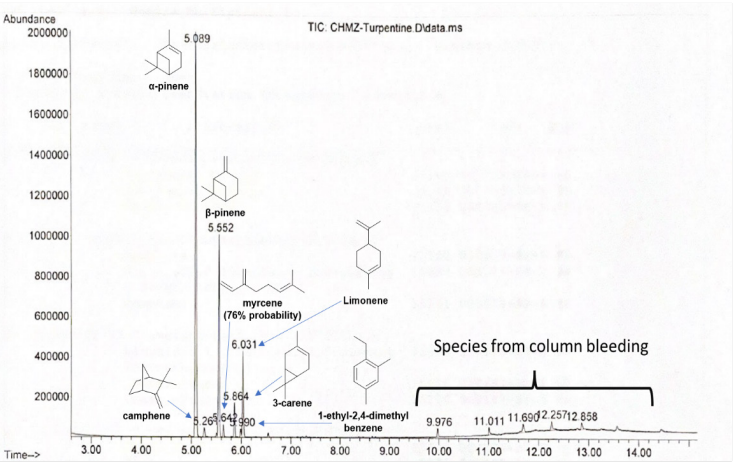

Figure 3. GC-MS chromatogram of turpentine

After receiving a sample of turpentine from Holmen Paper AB, GC-MS analysis was conducted to qualitatively determine the monoterpenes present within the mixture (**Fig. 3**). The three most abundant terpenes were α-pinene, β-pinene, and limonene. In our previous work in hydroaminoalkylation of commercially available terpenes, we identified β-pinene and limonene to be reactive in producing aminated terpenoids. [7] We were able to determine by ^{1}H NMR spectroscopy that reacting turpentine with N-methylaniline in the presence of our tantalum hydroaminoalkylation catalyst resulted in 72% amine consumption, 17% β-pinene consumption, and 48% limonene consumption (**Fig. 4**). These results re-affirm our previous published results using pure samples of β-pinene and limonene. We can conclude that our hydroaminoalkylation catalyst is able to selectively aminate terpenes in a mixture which streamlines our amination efforts with the terpene mixture extracts from the samples from Meadow Lake.

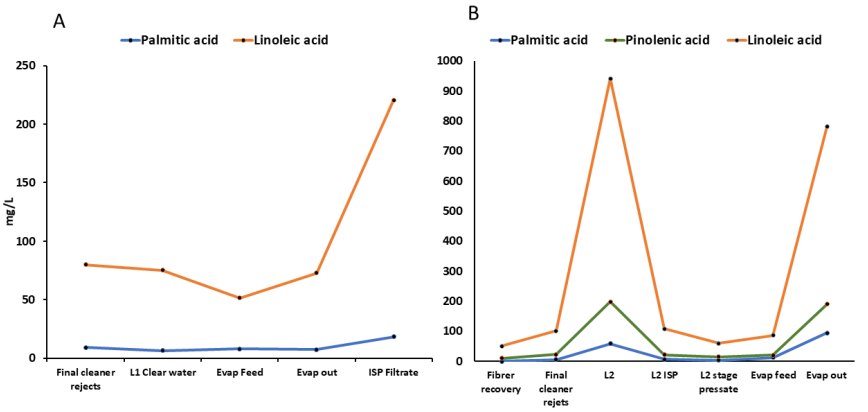

Figure 2. Fatty Acid Profile during Aspen operation (Panel A) and Softwood operation (Panel B)

PROJECT 2.2

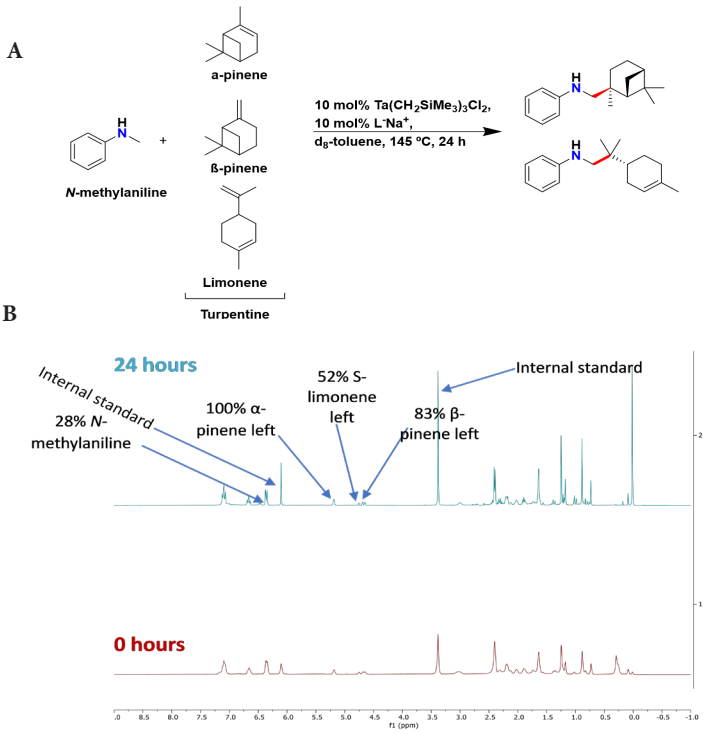

Figure 4. A) Reaction scheme for turpentine hydroaminoalkylation B)1H NMR spectrum of turpentine + N-methylaniline prior to heating (0 hours) and after heating (24 hours).

As a demonstration of our ability to evaluate anti-bacterial properties of the aminated terpenoid products, we conducted a disk diffusion assay (**Fig. 5**). In this assay, Methicillin-resistant Staphylococcus aureus (MRSA) was chosen to test anti-bacterial activity of the aminated turpentine mixture. For now, it appears that the turpentine mixture is not anti-bacterial. These results are a first investigation to biological testing and changes in parameters of the assay (e.g. sample loading, bacterial species, changing amine coupling partner) will be explored.

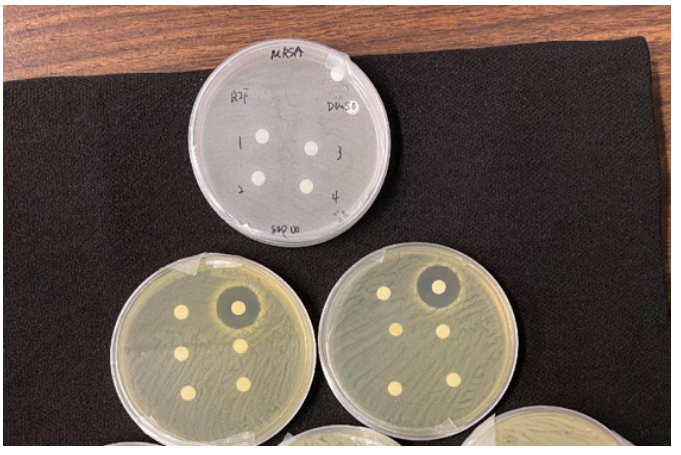

Future research

The next milestone will be to investigate the impact of pH on the recovery of fatty and resin acids in liquid and solid (pulp) samples. The identification and quantification of those extracts will enable us to determine the most promising samples for future valorization and develop odor control strategies. The extract enriched in fatty acids will be delivered to Professor Schafer's laboratory for decarboxylation and hydroaminoalkylation.

The characterization of extractives of adsorbed on fines will continue. The XPS and GC-MS profiles of extracts of fines will be compared to that of liquid samples to identify major compounds.

Regarding anti-bacterial screening, other bacteria and sample concentrations will be evaluated. As well, changing amine coupling partner allows for a library of aminated terpenoids deriving from turpentine to be developed.

References

1. Strömvall, A.-M.; Petersson, G., Terpenes emitted to air from TMP and sulphite pulp mills. Holzforschung 1992, 46, 99-102.
2. Valto, P.; Knuutinen, J.; Alén, R., Overview of analytical procedures for fatty and resin acids in the papermaking process. BioRessources 2012, 7 (4), 6041-6076.
3. Ström, G.; Stenius, P.; Lindström, M.; Ödberg, L., Surface chemical aspects of the behavior of soaps in pulp washing. Nordic Pulp & Paper Research Journal 1990, 5 (1), 44-51.
4. Tay, S., Effects of dissolved and colloidal contaminants in newsprint machine white water on water surface tension and paper physical properties. Tappi Journal 2001, 84 (8), 1-16.
5. McLean, D. S.; Vercoe, D.; Stack, K. R.; Richardson, D., The colloidal pKa of lipophilic extractives commonly found in Pinus radiata. Appita Journal 2005, 58 (5), 362-366.
6. Ziegleder, G., Volatile and Odorous Compounds in Unprinted Paperboard. Packag. Technol. Sci. 1998, 11, 231-239.
7. DiPucchio, R. C.; Rosca, S.; Athavan, G.; Schafer, L. L., Exploiting Natural Complexity: Synthetic Terpenoid-Alkaloids by Regioselective and Diastereoselective Hydroaminoalkylation Catalysis. ChemCatChem. 2019, 11 (16), 3871-3876.

Figure 5. Disk diffusion assay containing Methicillin-resistant *Staphylococcus aureus* (MRSA). Sample 1: turpentine, sample 2: aminated turpentine, sample 3: turpentine treated with catalyst, and sample 4: N-methylaniline treated with catalyst. Solvent control was loaded onto the top left disc, and positive control (antibiotic Rifampin) was loaded on the top right disc.

PROJECT 2.3

MFC PRODUCTION, CHARACTERIZATION, AND PROPERTIES OF MECHANICAL PULPS

Authors: Mariana Frias de Albuquerque, Samira Gharehkhani, Rasmita Sahoo, James Olson, Boris Stoeber, Heather Trajano

Background

This project aims to produce micro-fibrillated cellulose (MFC) from mechanically fractionated fines. In previous work it was demonstrated that LC refining of mechanical pulp can produce MFC capable of reinforcing TMP sheets. In this project we hypothesize that the natural microstructure of 'fines' subject to mechanical and enzymatic treatment will disassemble with little use of energy into an MFC suitable for reinforcement of high bulk, long-fibre TMP sheets, and that this MFC can be applied to the conventional TMP sheets to improve strength, surface, and barrier properties.

Since May, we have worked to develop a number of characterisation tools: gel point concentration, rheological characterisation, and high contrast stains for micro-CT imaging. Fines material has also been subjected to enzymatic hydrolysis.

Assessing Changes in Fibre Characteristics

a. Gel Point Concentration of MFC Suspension

In our previous report, we had begun exploring the use of gel point concentration to rapidly evaluate MFC quality without preparing handsheets. Gel point concentration of a fibre suspension is the lowest concentration at which the network can support load [1] and can be determined from a sedimentation test.

b. Rheological Characterisation of MFC Suspension

Our ultimate goal is to establish a relationship between fibre morphology and MFC rheology to achieve an online instrumentation for process control. The rheology of MFC suspension under shear flow provides insight into fibre and network structure. Rheology is influenced by fibre morphology (i.e., size and shape of fibrils) and surface chemistry (i.e., surface charge, and degree of hydrophilicity). The tendency of fibres to entangle and align creates complicated networks that display complex rheological behaviour. In general, MFC suspensions produced using different methods show different rheological behaviour [2].

Visualization

The challenge in micro-CT imaging of paper using MFC is to determine the distribution of MFC within the sheet. A potential solution is to stain or label MFC with heavy elements to enhance X-ray attenuation and thus contrast. Fundamentally, the contrast of X-ray images is dependent on the density, thickness, and atomic composition of the sample [3]. The use of contrast agents which contain heavy elements is widely accepted for conducting CT imaging. Identifying non-toxic and inexpensive contrast agents for simple staining protocols is of great interest [4]. The ionic compound, cesium iodide (CsI), seems to meet our requirements for contrast enhancement as both the cation and anion are heavy elements (Cesium: 57, Iodine: 52). MFC carries a negative charge on the surface, facilitating cation adsorption through electrostatic interactions. We hypothesize that Cs+ will adsorbed on the MFC surface while I- will diffuse into the MFC structure.

Enzyme Hydrolysis

Enzyme pretreatment is known to result in microfibres of desirable structure, size, and a higher aspect ratio than untreated MFC [5]. The greater the aspect ratio, the greater the reinforcement effect of MFC in composites. Endoglucanase is the most common enzyme used for MFC production. It targets specific bonds in cellulose, reducing fibre length and the degree of polymerization. Pääkkö et al. (2007) produced MFC of controlled nanoscale diameter and uniform size distribution with an endoglucanase pretreatment. The addition of even a mild enzyme hydrolysis step before shear degradation could significantly reduce costs associated with the required energy to produce MFC [6,7]. It is also possible that the enzyme step can affect the quality of subsequent composites and paper-based products containing the enzyme-treated MFC, as seen for example by Yoo and Hsieh (2010) who observed a substantial improvement in the tensile strength of paper and the production of thinner and less bright paper [8].

Literature cannot yet reliably predict the influence of enzyme treatment on MFC or lignin-rich MFC properties. Therefore, this project aims to evaluate the effect of enzymatic hydrolysis on the morphology of pulp fibres and on the properties of paper handsheets produced with them.

PROJECT 2.3

Results

Assessing Changes in Fibre Characteristics

a. Characterization by Gel Point Concentration

Previously, we reported gel point concentration (Φg) for short fibres obtained from bleached chemi-thermomechanical pulp (BCTMP) using a 1.0 mm smooth-holed screen. Results for refined material (below 700 kWh/t) were promising but not at higher levels of refining. Since June, we have evaluated the gel point concentration of MFC produced by refining short BCTMP fibres obtained using a 0.8 mm holed screen. Unfortunately, determination of gel point concentration did not provide insight on changes in MFC quality. We have decided that measuring Φg by sedimentation will not be further pursued as a characterisation tool.

b. Rheological Characterization of MFC suspension

Initial rheology testing was conducted with short BCTMP fibres recovered using 0.8 mm smooth-holed screen and no subsequent refining. Three fibre suspensions were prepared: 0.6, 1.0 and 1.4 wt%. Rheological measurements were performed by Kinexus rheometer with a 40 mm cone plate (CP 4/40) geometry at 25°C.

The shear rate dependent viscosity and shear stress of short fibre suspensions in Fig. 1 show three different regimes. At low shear rate, the fibre suspension appears to be unyielded with wall slip inside the rheometer. The appearent shear stress is 3 orders of magnitude larger at 1.4 wt% consistency as compared to 0.6 wt% most likely associated with the static yield stress of the 3D fibre network that is more prominent at higher concentation. As the shear rate increases beyond the plateau regime, the material appears to yield as the shear stress drops. The critical shear rate of this transition is higher for higher consistencies indicating that a larger shear force is required to break the strong fibre network. This transition in the flow curves at intermediate shear rates has been reported and observed with different measuring geometries such as plate-plate [2, 9]. This transition is likely associated with structural changes of the fibre network, which can be confirmed from rheomicroscopy images (future plan).

At higher shear rates, the fibre networks most likely break into many flocs and those flocs align parallel to the shear direction, while their flow curves approach each other.

Visualization

In all experiments, MFC suspension with a concentration of 0.3% was prepared and subjected to rigorous stirring to prevent agglomeration. Initial experiments were conducted using 0.15 mol/L CsI solution. This solution was added to the 0.3% MFC suspension and stirred at room temperature for 7 days. Paper sheets (60 g m^{-2}) were prepared with a small filtration system and a 5 cm diameter Whatman filter paper. After formation, the samples were dried at 105°C using a speed drier, separated from the filter paper, and stored in a desiccator.

Fig. 2a shows the CT scan image of the stained and unstained MFC papers. The stained MFC paper is brighter than the unstained MFC paper, showing improvement in contrast. Scanning Electron Microscopy (SEM) and Energy Dispersive X-ray analysis (EDX) were also conducted (Fig. 2 b-d). Fig. 2d indicates that CsI was evenly distributed on the surface. The detection of Cs+ and I- was also confirmed by EDX.

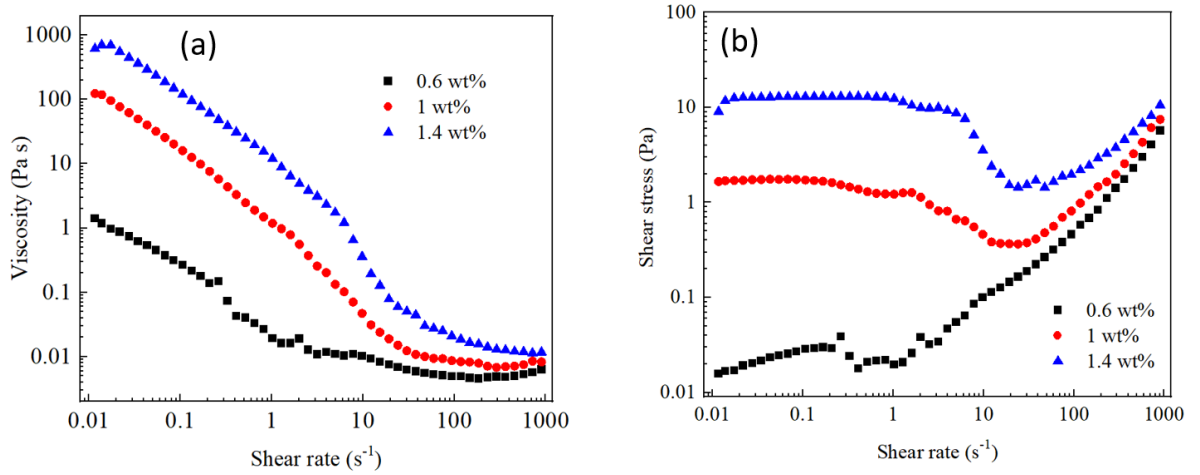

Figure 1. (a) Shear viscosity as a function of shear rate. (b) Shear stress as a function of shear rate at different concentrations of pulp fibre. Fibres were obtained using a 0.8 mm smooth-holed screen and were not subjected to refining.

PROJECT 2.3

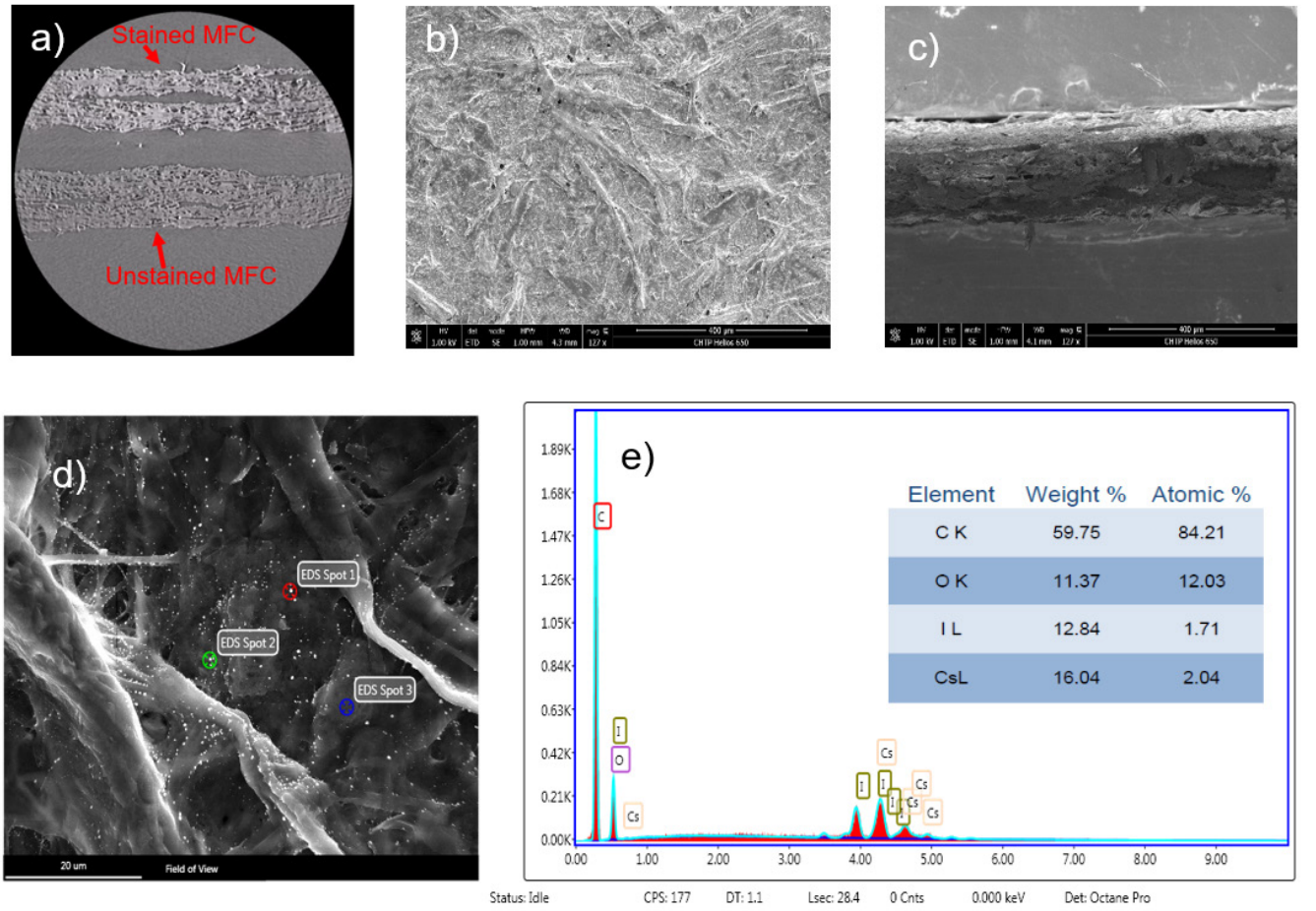

Figure 2. a) CT scan image of paper made from CsI-stained and unstained MFC at 60 kV, b) and c) SEM image of surface and cross-section of paper made from CsI-stained MFCs, d) and e) EDX results for the paper made from CsI-stained MFCs.

Enzyme Hydrolysis

Enzymatic hydrolysis was conducted at 50°C for 2 hrs. The 2 wt% fibre suspension was prepared with short fibres obtained by using 0.8 mm smooth-holed screen. The enzyme dosage was 10 wt% of the oven-dried mass of pulp. Fibre suspension samples were exposed to endoglucanase (ARL), exoglucanase (3068), and mannanase (EL 2021/003712) as well as a 50:50 mixture of endoglucanase and mannanase. In addition, a reference sample was subjected to incubation without enzyme addition. The length and width of the fibres were evaluated using the FQA after enzymatic hydrolysis or incubation. These initial results are depicted in Table 1.

Compared to the reference sample, fibre width was not significantly affected by enzymatic treatment. This is understandable, given that enzymatic activity acts to "cut" cellulose, reducing polymer length. There was a small reduction in fibre length following enzymatic hydrolysis. The most significant reduction, approximately 7%, came from endoglucanase application. The smallest reduction, approximately 1%, was from mannanase application. We will shortly obtain FQA data after refining the enzyme-treated fibres in the PFI mill.

Table 1. Fibre length and width obtained from FQA after enzyme hydrolysis

Sample	Fibre length (mm)	Width (μm)
Endoglucanase	0.948 ± 0.020	31.15 ± 0.21
Endoglucanase + Mannanase	0.988 ± 0.008	31.50 ± 0.42
Exoglucanase	0.993 ± 0.022	31.05 ± 0.21
Mannanase	1.007 ± 0.020	30.80 ± 0.42
Reference	1.018 ± 0.007	31.00 ± 0.57

PROJECT 2.3

Future research

Assessing Changes in Fibre Characteristics

The rheology of MFC suspensions produced with different specific energies and enzyme treatments will be determined using rheomicroscopy. The rheological properties of MFC suspension will be related to MFC images as well as handsheet properties such as tensile index.

Visualization

We will stain alkaline-treated MFC with CsI in order to determine the effect of MFC charge on adsorption. In another set of experiments, we will work on the use of osmium and silver decoration as staining agents. Finally, we will extend our work towards visualization of paper handsheets made from mixtures of MFC and long fibres in order to understand the distribution of MFC in such composites.

Enzyme hydrolysis

The next steps of the project consist of a systematic study of the effect of different enzymes on the fibrillation of pulp fibres. This study will consider the dosage, type of enzymes used, and exposure time.

References

1. Martinez, D. M., Buckley, K., Jivan, S., Lindstrom, A., Thiruvengadaswamy, R., Olson, J. A., Ruth, T. J., & Kerekes, R. J. (2001). Characterizing the mobility of papermaking fibres during sedimentation. The Science of Papermaking: Transactions of the 12th Fundamental Research Symposium, Oxford. The Pulp and Paper Fundamental Research Society, Bury, UK, 225–254.
2. Agoda-Tandjawa, G., Durand, S., Berot, S., Blassel, C., Gaillard, C., Garnier, C., & Doublier, J.-L. (2010). Rheological characterization of microfibrillated cellulose suspensions after freezing. Carbohydrate Polymers, 80(3), 677–686.
3. Lusic, H., & Grinstaff, M. W. (2013). X-ray-computed tomography contrast agents. Chemical Reviews, 113(3), 1641–1666.
4. Wang, Z., Verboven, P., & Nicolai, B. (2017). Contrast-enhanced 3D micro-CT of plant tissues using different impregnation techniques. Plant Methods, 13(1), 1–16.
5. Henriksson, M., Henriksson, G., Berglund, L. A., & Lindström, T. (2007). An environmentally friendly method for enzyme-assisted preparation of microfibrillated cellulose (MFC) nanofibers. European Polymer Journal, 43(8), 3434–3441. https://doi.org/10.1016/j.eurpolymj.2007.05.038
6. Pääkkö, M., Ankerfors, M., Kosonen, H., Nykänen, A., Ahola, S., Österberg, M., Ruokolainen, J., Laine, J., Larsson, P. T., & Ikkala, O. (2007). Enzymatic hydrolysis combined with mechanical shearing and high-pressure homogenization for nanoscale cellulose fibrils and strong gels. Biomacromolecules, 8(6), 1934–1941.
7. Hu, J., Tian, D., Renneckar, S., & Saddler, J. N. (2018). Enzyme mediated nanofibrillation of cellulose by the synergistic actions of an endoglucanase, lytic polysaccharide monooxygenase (LPMO) and xylanase. Scientific Reports, 8(1), 1–8.
8. Yoo, S., & Hsieh, J. S. (2010). Enzyme-Assisted Preparation of Fibrillated Cellulose Fibers and Its Effect on Physical and Mechanical Properties of Paper Sheet Composites. Industrial & Engineering Chemistry Research, 49(5), 2161–2168. https://doi.org/10.1021/ie901621n
9. Karppinen, A., Saarinen, T., Salmela, J., Laukkanen, A., Nuopponen, M., & Seppälä, J. (2012). Flocculation of microfibrillated cellulose in shear flow. Cellulose, 19(6), 1807–1819.

PROJECT 3.1

CREATING BULKY FIBRES

Authors: Elisa Ferreira, Emily Cranston, Mark Martinez

Background

During papermaking processes, fibre collapse readily occurs, causing a reduction in the lumen volume [1,2]. This project aims to increase bulk (or decrease fibre collapse) at a prescribed tensile strength through novel surface modification routes. One means to prevent collapse is by reducing the interfacial tension inside the lumen with hydrophobic surface functionalization. As a first step, we are developing tools to analyse fibres by X-ray micro-computed tomography (μCT), which will allow for the evaluation of fibre morphology and fibre-fibre bonds as a function of different surface chemistries.

In the μCT analysis, a specimen is exposed to an X-ray beam that scans the sample volume. The intensity of the X-ray beam is attenuated as the waves penetrate the sample. In sequence, the attenuated radiation is detected as a 2D projection of the specimen. Several 2D projections are collected from the specimen, such that these images can be reconstructed into a 3D model. The process of X-ray attenuation depends on the attenuation coefficient of the elements presented in the sample [3]. Cellulose fibres are primarily composed of organic compounds that have a low attenuation coefficient in the range of the X-ray energies used in μCT. As fibre materials cannot attenuate X-rays efficiently, μCT scans of fibre networks generate images with a low contrast in which detailed fibre analysis is challenging.

We propose to deposit inorganic particles on fibre surfaces as agents to enhance contrast (i.e., labels) in μCT imaging. A similar approach was previously demonstrated with cellulose nanofibers (CNFs) and fibre fragments decorated with $CoFe_2O_4$ nanoparticles [4]. The nanoparticles were applied as labels for μCT analysis, enabling the identification of CNFs and fibre fragments in a paper network. Using this approach, nano and microstructures of cellulose could be labelled successfully; however, the yield and the efficiency of the method was low, particularly on fibres. Therefore, $CoFe_2O_4$-labelled fibres could not be identified by μCT analysis [4]. We have attempted to reproduce the $CoFe_2O_4$-labelling in CTMP (chemi-thermomechanical pulp) fibres. The presence of $CoFe_2O_4$ nanoparticles enhanced the contrast of the μCT image; however, the inorganic layer could not be distinguished from fibres. As the synthesis of $CoFe_2O_4$ is controlled by several parameters and the attenuation coefficients of iron and cobalt are equivalent, we proposed the application of Fe_2O_3 as an alternative contrast agent for μCT analysis. Hereby, we developed a protocol to produce Fe_2O_3 nanoparticles *in situ* on the fibre surface, forming a uniform particle layer, which generated high contrast in μCT images.

Experimental work

Fe_2O_3-labelling: The R14 fraction of a CTMP (length ~3.5 mm) were dispersed at 0.1% consistency in a solution of 0.18 mol/L $FeSO_4$ at 90 °C for 3 h. After soaking the fibres, the supernatant was removed, and the fibres were re-dispersed in water. A solution of NaOH was added into the flask at a final concentration of 0.54 mol/L and system was kept at 90 °C for 3 h. After the precipitation, fibres were rinsed with water until neutral pH. Handsheets were prepared from labelled fibres dispersed in water by vacuum filtration and drying at 105 °C.

Results

The method used to label the fibres had two steps: (1) impregnation of fibres with an aqueous solution with iron ions, and (2) precipitation of iron species by increasing the pH. The formation of Fe_2O_3 nanoparticles occurred as a consequence of the low solubility of Fe3+ in alkaline pH [5]. After the reaction, Fe2O3-labelled fibres were brown, which indicates that iron nanoparticles were successfully produced in situ on the fibre surface (Figures 1a-d). Moreover, images from scanning electron microscopy (SEM) revealed the presence of Fe_2O_3 nanoparticles with a diameter of approximately 250 nm, distributed fairly evenly on the fibre surface (Figures 1f-h).

PROJECT 3.1

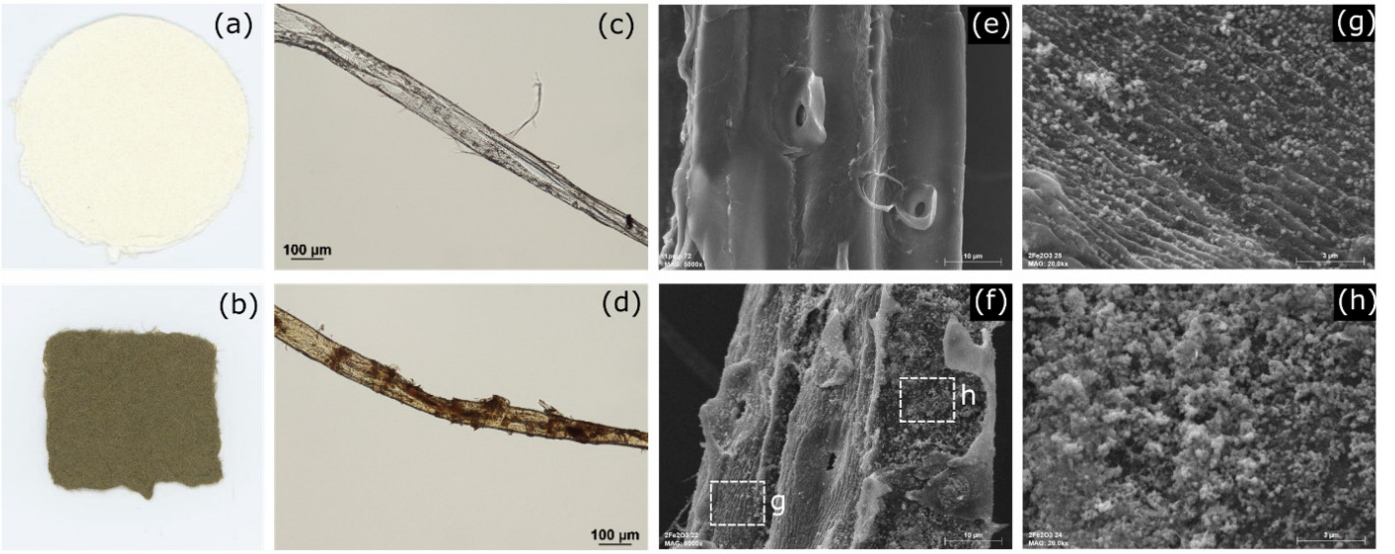

Figure 1. Macroscopic view of CTMP handsheets prepared with: (a) unlabelled fibres (control); (b) Fe_2O_3-labelled fibres. Images from optical microscopy and SEM from: (c,e) unlabelled pulp fibres; (d,f-h) Fe_2O_3-labelled fibres. Details on fibre surface in (f) illustrated the presence of Fe_2O_3 nanoparticles with an average diameter of 250 nm, which were distributed as (g) monolayers and (h) aggregates.

Fe_2O_3-labelled fibres were analysed by µCT from which a high contrast was produced, illustrating that Fe_2O_3 particles can be applied as labels to visualize the fibre surface (Figure 2). The surface modification of fibres with Fe_2O_3 nanoparticles for µCT analysis is a novel approach that is being further optimized to study the morphology and properties of fibre networks.

Future research

In the next steps, we will investigate the role of morphology and composition in µCT imaging by analysing fibre samples with a range of Fe_2O_3 contents. Nano and microstructures of labelled fibres will be examined by SEM and the composition will be quantified by energy dispersive spectroscopy (EDS-SEM). Ultimately, we will apply Fe_2O_3 (and other metal nanoparticle) labels to characterize the structure and properties of bulky fibres with a range of surface chemistries. For future research, our goals are to use labelled fibres as a model to investigate fibre-fibre bonds from bulky fibres with different surface chemistries by µCT analysis. Furthermore, the characterization tools that we are developing are promising to evaluate mechanical properties of fibre materials and their dynamics in water through *in situ* testing coupled with µCT.

Acknowledgements

The authors thank Jacob Kabel and the Electron Microbeam and X-Ray Diffraction Facility (EMXDF-UBC) for SEM facility and training.

References

1. Mark, R. E., Borch, J., & Habeger, C. (2002). Handbook of Physical Testing of Paper (Vol. 1). Marcel Dekker.
2. Yamauchi, T. (2007). A method to determine lumen volume and collapse degree of pulp fibers by using bottleneck effect of mercury porosimetry. Journal of Wood Science, 53(6), 516–519.
3. Boerckel, J. D., Mason, D. E., McDermott, A. M., & Alsberg, E. (2014). Microcomputed tomography: approaches and applications in bioengineering. Stem cell research & therapy, 5(6), 144.
4. Hobisch, M. A.; Zabler, S.; Bardet, S. M. et al. How cellulose nanofibrils and cellulose microparticles impact paper strength—A visualization approach. Carbohydr. Polym. 2021, 254, 117406.
5. Cornell, R. M.; Giovanoli, R.; Schneider, W. (1989) Review of the hydrolysis of iron (III) and the crystallization of amorphous iron-(III) hydroxide hydrate. J. Chem. Technol.

PROJECT 3.2

ADVANCED CHARACTERIZATION – COMPUTED TOMOGRAPHY

Authors: Aurélien Sibellas, James Drummond, Samuel Brown, Mark Martinez, André Phillion

Background

X-ray microcomputed tomography is a non-destructive technique to acquire 3D grayscale images of objects at the microscopic scale [1]. It opens a wide range of investigations of the inner structure of wood and paper handsheets and enables a better understanding of the relationship with their final physical properties. The last four months were devoted to studies of:

- The effect of chemical impregnation and axial compression on the microstructure of wood chips (supporting Project 1.3).
- The effect of LC refining and/or MFC addition on the microstructure of mechanical pulp handsheets (supporting Project 2.3 and 3.1).

Project 1 – Maximizing the Bulk Potential of Mechanical Pulps

The vision of this work is to maximize and preserve bulk during the mechanical pulping process. In this project we examine different chemical treatments of wood chips and measure the response of the wood matrix to mechanical load, approximating the refining treatment. Over this reporting period, we visualized the axial compression of a wood chip using computed tomography.

Scanning conditions for wood at rest (Figure 1a) are now well-understood, giving high resolution images with good contrast between phases (Air and wood cell walls) as seen in Figure 1b. A new image processing code was developed to extract structural properties from the original 3D grayscale images of wood chips: an efficient algorithm for cell wall segmentation and lumen labelling is performed (Figure 1c) to get each individual fibre and their centroid. The approach was applied on chemically treated aspen wood chips: treatments were carried out with either sodium sulfite (0.4 M pH10, or, 1 M pH12), alkaline peroxide (pH 13), or water (control). Tomography images were obtained at a resolution of 0.7 µm (note that cell wall thickness is ~6µm). Initial results have shown that the ratio of lumen area to wall thickness is constant independent of the chemical treatment. Therefore, no significant change has been observed in the structure at the studied scale. However, changes can occur at a lower scale, e.g. at a tenth or a hundredth of the pixel size used.

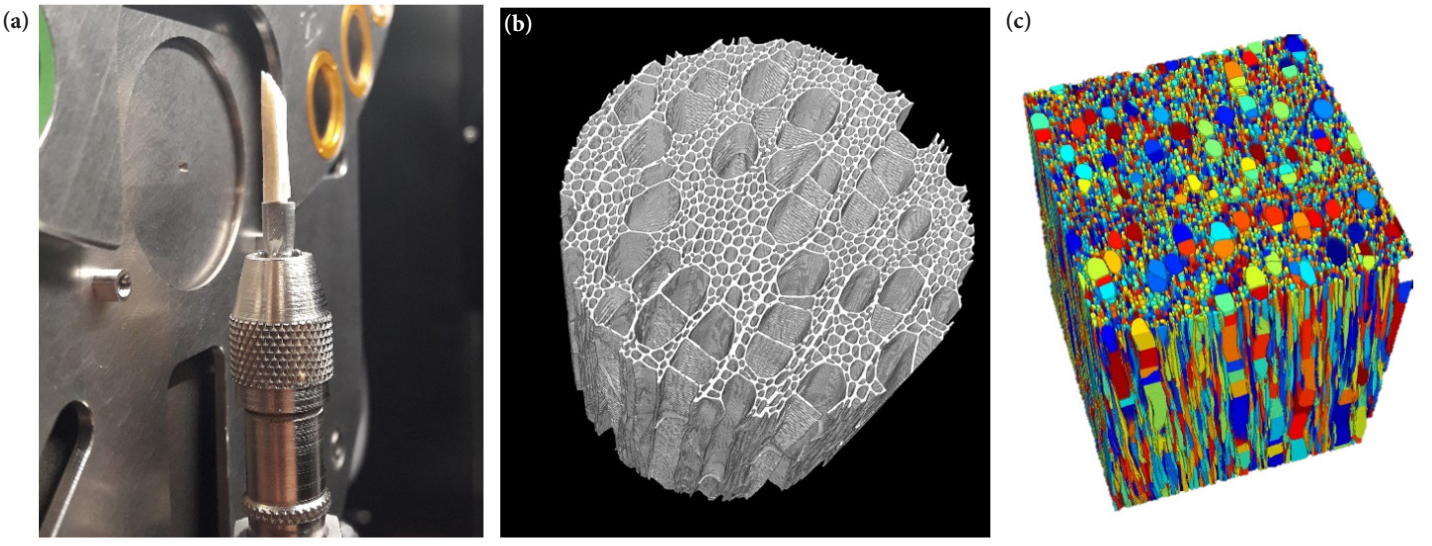

Figure 1. (a) A wood chip sample is mounted on a pin in front of the X-ray beam output. (b) 3D rendering of aspen wood chip at rest. (c) A new image processing code has been developed to label each individual lumen in the wood structure.

PROJECT 3.2

A complete in-situ axial compression test (in the direction of the tracheids) of an aspen wood chip has been carried out at a resolution of 1.2 µm, giving a 3D image for each of the 11 steps (compression displacement step of 60 µm), from an undeformed state to a 10% compressed relative to initial sample height. A smaller in-situ compression device was designed (Figure 2) to allow higher resolution and decreased scanning time (6 hours for each step for a total of 60 hours of tomography time. This first investigation showed a very limited depth (about 80 µm) of buckling of wood cells, and quantitative analysis of the lumen centroids may bring answers as to the buckling mechanism(s). Furthermore, Digital Volume Correlation (DVC) analysis confirmed that compression occurs in the cell walls prior to buckling and crushing. Further in-situ mechanical tests on wood chips can now be performed and combined with very efficient data extraction algorithms for dynamic wood structure characterization.

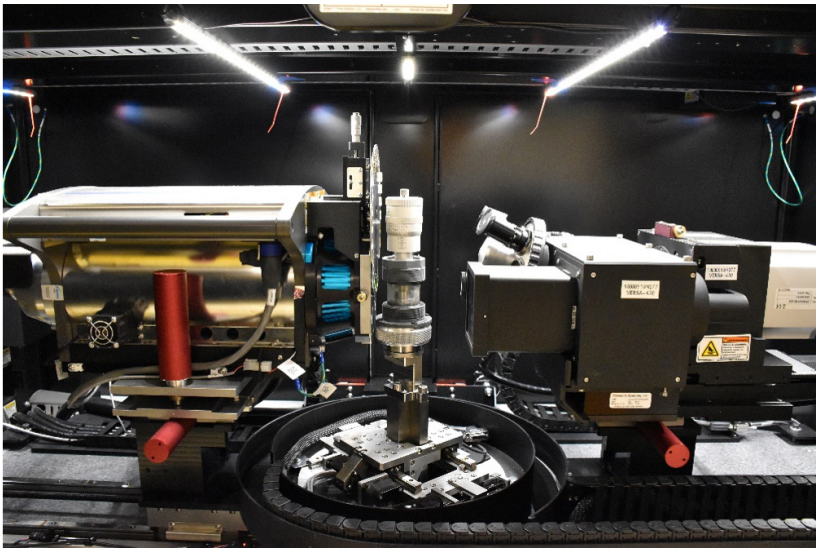

Figure 2. A smaller compression device (in the middle) has been designed to carry out in-situ compression of wood chips with higher resolution, lower level of noise and enhanced image contrast.

Project 2 – Imaging paper handsheets

The vision of this project is to gain insight into the microstructure of mechanical pulp handsheets at different MFC and LC refining levels. A key step before beginning the process of quantifying microstructural properties from images is the development of an imaging protocol that balances resolution, sampling time, and image quality. Although the optimal parameters have been obtained through systematic investigations, image contrast between phases (air and fibre walls) remains poor, as expected with biological samples. In more recent work, contrast has been improved using different metal coatings, as metal x-ray attenuation coefficients are higher than polymers and air. Two approaches have given encouraging results: nanoparticle fibre decoration using Iron and an osmium tetroxide coating enhanced with Uranyl acetate and lead citrate. Although fibre nanoparticle decoration is a layer of around 50 nm thickness, much less than the pixel size, image contrast has been improved leading to well-defined fibre morphology and cell wall cross-sections as depicted in Figure 3.

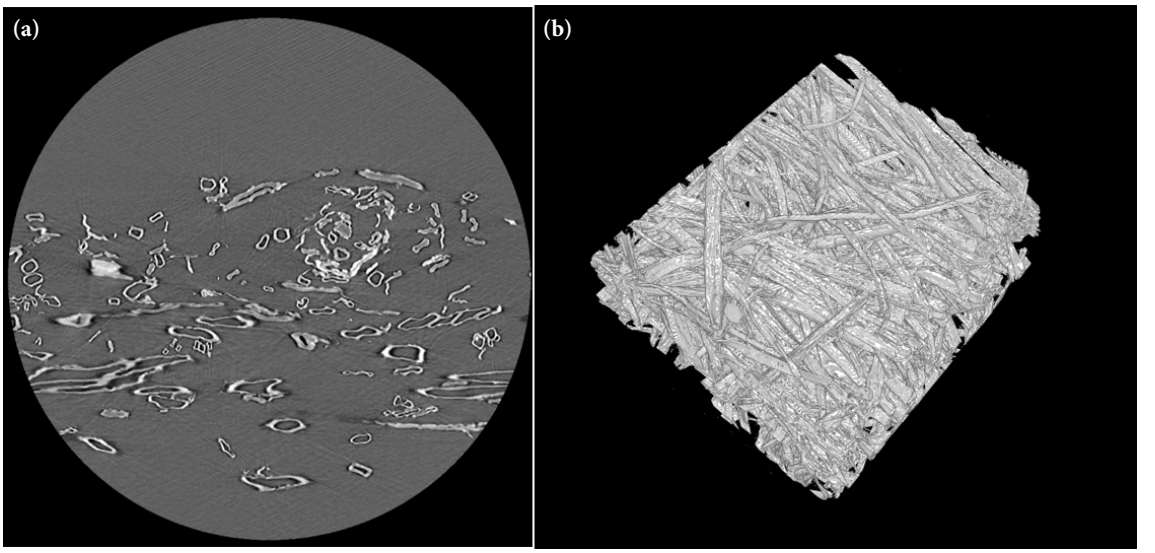

Figure 3. (a) Paper sheet cross-section with Fe nanoparticle decoration on fibres. Better contrast is obtained (phases have distinct gray values) which considerably simplifies the segmentation procedure. (b) 3D rendering of the paper sheet after filtering and segmentation.

PROJECT 3.2

Investigations of object contacts in images from tomography has continued in parallel. An original robust method of counting the contacts between spherical particles is now operational and lays the foundation for handling contacts in heterogeneous polydisperse assemblies of particles. Previously, random monodisperse assemblies of nylon fibres have been analyzed with the new method and the number of contacts per particles is reported in Figure 4. A comprehensive investigation of these kinds of structures will help confirm theoretical models that didn't receive experimental support, and can be extended to paper handsheets as it impacts their physical properties.

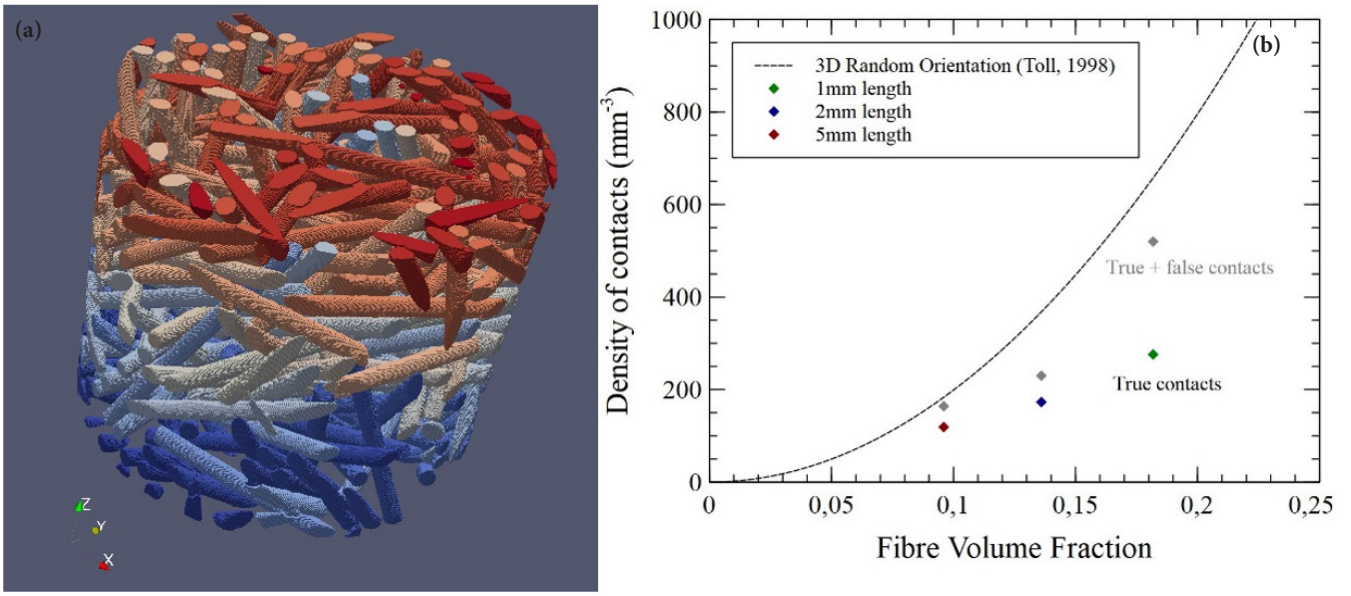

Figure 4. (a) Random assembly of nylon fibres. (b) The density of contacts is plotted versus the fibre volume fraction with the new method for counting the contacts. Experimental results for different fibre lengths show a lower value than predicted by Toll's model.

Future research

Over the past five months, 3D dynamic image acquisition of wood has been combined with new image processing algorithms able to extract meaningful data: the wood structure can be followed and characterized by lumen tracking over numerous compression steps. Those results will be compared to Digital Volume Correlation, a powerful method which will help to get a precise characterization of the buckling mechanism of the wood cells. As data extraction is now feasible for paper handsheets, efforts have focused on image contrast enhancement with encouraging results obtained from nanoparticle decoration. Systematic investigations will identify the optimal parameters, and characterization of the coating morphology will be performed with classical microscopy techniques.

References

1. Buffière, J.-Y., Maire, E., Adrien, J., & Masse, J.-P. (2010). In Situ Experiments with X ray Tomography : An Attractive Tool for Experimental Mechanics. Experimental Mechanics, 50, 289–305. https://doi.org/10.1007/s11340-010-9333-7

ERMP PERSONNEL UPDATES

FAREWELLS

Recently the ERMP group has said farewell to one of our best team players and Laboratory Technician Reanna Seifert. Reanna left the PPC end of September and moved to the island to start a new position as a Fire Assay Technician at Blue Coast Research, in Parksville. Blue Coast Research is a mining consultancy company working with existing mining operations and new exploration sites to extract the precious metals. We wishes the best to Reanna on this new path, and thank her for all the great contributions on the past 5 years to the ERMP program. You will be missed Reanna!

Reanna in Nanoose Bay.

NEW ARRIVALS

We continue welcoming several new team members at the UBC Pulp and Paper Center. Please read through the brief introductions of our new team members and their backgrounds.

Norman Roberts

New Laboratory Technologist based at the PPC, Norman holds a, Diploma in Engineering (Honours), in Mechanical and Electrical Engineering from Harare Polytechnic, Zimbabwe. He brings many years of experience from FPInnovations, in the areas of low consistency pulp refining and screening and also in the development of novel cellulose fibre-reinforced bio-products.

Norm collaborates with ERMP researchers on low consistency refining and is responsible for processing and testing of samples in the PPC papermaking lab. He is also responsible for training the ERMP Work Learn students and supervises their work. With Reanna's departure, Norm is taking over her responsibilities by managing the papermaking lab, and assisting in the refining trials.

Norm at the High Head Lab at the PPC.

Samuel Brown

Sam joined the ERMP team as a co-op student in September 2021. He is currently pursuing a BSc in Physics at UBC, and has experience in optics, image processing, and scientific computing. In previous co-op terms, Sam worked as a fuel cell test engineer at Ballard Power Systems and as a biophysics researcher at the Université de Montréal Biophotonics Lab. During his 4 months here, he will be supporting Project 3.2 with image analysis of wood chip compression effects.

ERMP PERSONNEL UPDATES

Dua E Naqvi

Dua is an undergraduate Co-op student working with the ERMP team since September 2021. She is currently working in a number of projects at the PPC related to bio-based materials, as well as assisting researchers in the papermaking lab. She is in her fourth-year of the BASc in Chemical Engineering program at UBC, and doing a Minor in Creative Writing. Her interests include sustainability, clean energy and waste reduction

Upcoming Event

Our next ERMP Steering Committee Meeting will be held in November 16th, from 8 am PST to 12.30 pm PST through the Zoom platform.

All ERMP Steering Committee members are invited for lunch at CHBE 202 from 1 pm after attending the Zoom meeting.

PPC UPDATES

LAB UPDATES

A brand new horizontal tester from Messmer Büchel is now available at the Pulp and Paper Center to complement our existing L&W testing machine. This 84-56 Horizontal Tensile Tester has a 250 N load cell and will facilitate data collection as test results can now be displayed and transmitted via USB output. prior to this, users would print the test results and type data individually which was quite time consuming. The data can be used with the TMI Graph master data acquisiton system to graph and store directly into our PC.

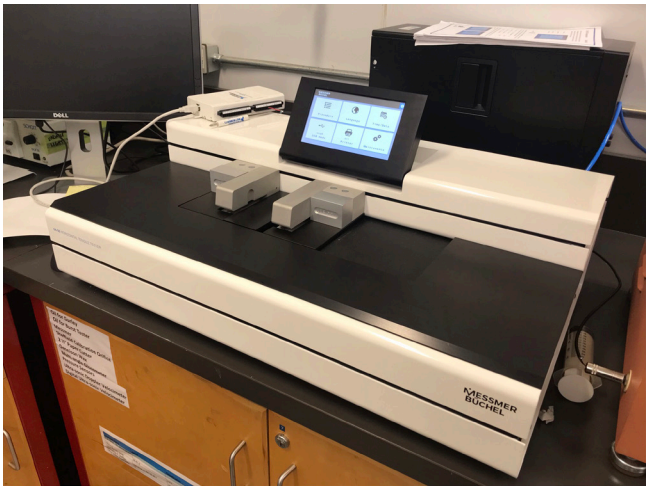

New Horizontal tester at the CTH room, PPC - UBC.

TRIAL UPDATES

Early this summer, we received some new BCTMP pulp bales from West Fraser, Quennel River pulp to continues studies on project 2.3 and other ERMP projects. Additionally, we also received a couple of aspen pulp bales directly from Meadow Lake to compare pulp furnishes. During September, we carried out some new refining and fractionation trials (with 0.8 mm screen) to compare performances and create a new baseline for the BCTMP pulp. We thank West Fraser-QRP and Meadow Lake for the in-kind contributions to the program.

George Soong and Reanna Seifert at the HHL during fractionation trials.

PUBLICATIONS

Conferences and Seminar

Aurélien Sibellas. " Estimating the number of contacts in sedimented fibre assemblies". Presented at the 2021 Progress in Paper Physics Seminar held online on October 7th, 2021.

Journal Articles

Aigner, Matthias, Olson, James, Sun, Yu and Wild, Peter. "Interpretation of force profiles in mill-scale LC refining" Nordic Pulp & Paper Research Journal, vol. , no. , 2021, pp. 000010151520210058. https://doi.org/10.1515/npprj-2021-0058

NEWS - FROM OUR PARTNERS

We want to congratulate Ali Elahimehr and Yu Sun, both former ERMP team members, on winning the Top 10 Under 40 Program on Pulp & Paper Canada for 2021.

Ali Elahimehr joined the initial phase of the program as a Ph.D. student working closely with Professors James Olson and Mark Martinez in better predicting pulp properties from low consistency refiner operating conditions. After graduation in 2013, Ali continued working as a Process Engineer with West Fraser, Quesnel River Pulp, to evaluate existing processes to reduce energy costs and efficiencies. Nowadays, Ali works as a Senior Scientist in development and implementation at FPInnovation and continues to participate in the ERMP consortium as one of the representatives from FPInnovation.

Ali Elahimehr

Yu Sun was a Postdoctoral Research Fellow with the ERMP program from 2014 to 2017 under the supervision of Rodger Beatson at BCIT. Her work focused on determining the chemical charges and pre-treatment conditions required across the mechanical pulping process to obtain desired pulp properties at the lowest energy and cost. Currently, Yu Sun manages the TMP & stock prep department at Catalyst Paper's Crofton Mill on Vancouver Island.

More details on, the Pulp & Paper Canada website.

Yu Sun

CONTACTS

You are welcome to contact any of the faculty or staff:

Daniela Vargas Figueroa
Program Manager, UBC
604-827-2390
Daniela.Figueroa@ubc.ca

Mark Martinez
Professor, UBC
604-822-8564
Mark.Martinez@ubc.ca

James Olson
Professor, UBC
604-822-5705
James.Olson@ubc.ca

Rodger Beatson
Professor, BCIT
604-432-8951
Rodger_Beatson@bcit.ca

Laurel Schafer
Professor, UBC
604-822-9264
Schafer@chem.ubc.ca

Peter Wild
Professor, UVic
250-721-8901
PWild@uvic.ca

Bhushan Gopaluni
Professor, UBC
604-827-5668
Bhushan.Gopaluni@ubc.ca

Emily Cranston
Associate Professor, UBC
604-827-0627
Emily.Cranston@ubc.ca

Boris Stoeber
Professor, UBC
604-827-5907
Boris.Stoeber@ubc.ca

Heather Trajano
Associate Professor, UBC
604-827-1823
Heather.Trajano@ubc.ca

Yankai Cao
Assistant Professor, UBC
604-822-2693
Yankai.Cao@ubc.ca

Scott Renneckar
Associate Professor, UBC
604-827-0637
Scott.Renneckar@ubc.ca

André Phillion
Associate Professor, McMaster
905-525-9140 x24046
Philliab@mcmaster.ca

Visit our website www.EnergyReduction.ppc.ubc.ca

PARTNERSHIP IS OUR STRENGTH

The supporting partners of this research program are:

AB Enzymes, Alberta Newsprint Company, BC Hydro, BCIT, Canfor, Catalyst Paper, FPInnovations, Holmen Paper, McMaster University, Meadow Lake Pulp, Millar Western, NSERC, The University of British Columbia Pulp and Paper Centre, The University of Victoria, West Fraser and Valmet.